

1 **Who were the Nataruk people? Mandibular morphology among late Pleistocene and early**
2 **Holocene fisher-forager populations of West Turkana (Kenya).**

3 Aurélien Mounier^{1,2}, Maria Correia², Frances Rivera², Federica Crivellaro², Ronika Power^{2,3}, Joe
4 Jeffery², Alex Wilshaw², Robert A. Foley^{2,4}, Marta Mirazón Lahr^{2,4*}.

5

6 ¹UMR 7194, CNRS-Muséum national d'Histoire naturelle, Musée de l'Homme, 17 place du Trocadéro
7 et du 11 novembre, 75016 Paris, France.

8 ²Leverhulme Centre for Human Evolutionary Studies, Department of Archaeology and Anthropology,
9 University of Cambridge, Fitzwilliam Street, Cambridge CB2 1QH, United Kingdom.

10 ³Department of Ancient History, Level 5, W6A Building, Macquarie University, NSW 2109, Australia

11 ⁴Turkana Basin Institute, Kenya

12

13 *Corresponding author: Marta Mirazón Lahr

14 e-mail: mbml1@cam.ac.uk

15

16

1 Abstract

2 Africa is the birthplace of the species *Homo sapiens*, and Africans today are genetically more diverse
3 than other populations of the world. However, the processes that underpinned the evolution of
4 African populations remain largely obscure. Only a handful of late Pleistocene African fossils (~50-12
5 Ka) are known, while the more numerous sites with human fossils of early Holocene age are patchily
6 distributed. In particular, late Pleistocene and early Holocene human diversity in Eastern Africa
7 remains little studied, precluding any analysis of the potential factors that shaped human diversity in
8 the region, and more broadly throughout the continent. These periods include the Last Glacial
9 Maximum (LGM), a moment of extreme aridity in Africa that caused the fragmentation of population
10 ranges and localised extinctions, as well as the 'African Humid Period', a moment of abrupt climate
11 change and enhanced connectivity throughout Africa. East Africa, with its range of environments,
12 may have acted as a refugium during the LGM, and may have played a critical biogeographic role
13 during the heterogeneous environmental recovery that followed. This environmental context raises
14 a number of questions about the relationships among early Holocene African populations, and about
15 the role played by East Africa in shaping late hunter-gatherer biological diversity. Here, we describe
16 eight mandibles from Nataruk, an early Holocene site (~10 Ka) in West Turkana, offering the
17 opportunity of exploring population diversity in Africa at the height of the 'African Humid Period'.
18 We use 3D geometric morphometric techniques to analyse the phenotypic variation of a large
19 mandibular sample. Our results show that (i) the Nataruk mandibles are most similar to other
20 African hunter-fisher-gatherer populations, especially to the fossils from Lothagam, another West
21 Turkana locality, and to other early Holocene fossils from the Central Rift Valley (Kenya); and (ii) a
22 phylogenetic connection may have existed between these Eastern African populations and some
23 Nile Valley and Maghrebian groups, who lived at a time when a Green Sahara may have allowed
24 substantial contact, and potential gene flow, across a vast expanse of Northern and Eastern Africa.

25

26 *Keywords:* Late human evolution; Africa; Nataruk; West-Turkana; mandibles; phenetic

27

1 Introduction

2 Africa is the birthplace of our species, *Homo sapiens*, from where all human populations diversified.
3 The earliest fossils that show the unique, universal characteristics of a modern human morphology
4 are found in East Africa 200,000 – 160,000 years ago (Ka) (Day, 1969; Leakey, 1969; White et al.,
5 2003; Fleagle et al., 2008), while recent proposals for an earlier origin for the species would extend
6 this date to ca. 300 Ka (Hublin et al., 2017). Africans today are genetically more diverse than other
7 populations of the world, reflecting the population size and time-depth of modern human presence
8 in the continent (Liu et al., 2006; Li et al., 2008). Genetic data further point to significant population
9 change associated with the expansion of food-producing populations in the last 4000 years (Tishkoff
10 et al., 2009). However, between these two extremes in time, the historical, ecological and adaptive
11 processes that underpinned the evolution of African populations remain largely unknown. Only a
12 handful of late Pleistocene sites (~50-12 Ka) with human remains are known (Grine, 2016), and these
13 are mostly located in North or South Africa. This period includes the Last Glacial Maximum, a
14 moment of extreme aridity in Africa (Gasse, 2000; Clark et al., 2009) that caused the fragmentation
15 of population ranges and localised extinctions. East Africa, with its diversity of environments and
16 high relief, may have acted as a refugium (Mirazón Lahr and Foley, 2016), thus playing a critical
17 biogeographic role within the continent during phases of late Pleistocene aridity. Contrastingly, the
18 early-to-mid Holocene (12-5 Ka) – the ‘African Humid Period’ (AHP) – was a moment of abrupt
19 climate change (deMenocal et al., 2000) and enhanced connectivity throughout Africa, including the
20 expansion of productive biomes and greening of the Sahara (Larrasoaña et al., 2013). However, the
21 timing of environmental recovery was not synchronous throughout the continent (Carolin et al.,
22 2013), creating the opportunity for the differential expansion of those populations who first
23 experienced ameliorated conditions (Mirazón Lahr, 2016). This environmental context raises a
24 number of questions about the relationships among early Holocene African populations and, in
25 particular, about the role played by East Africa in shaping late hunter-gatherer biological diversity in
26 the continent. The number of sites and human fossil remains of early Holocene age in Africa is
27 greater than earlier phases, but these are patchily distributed. In particular, the late Pleistocene and
28 early Holocene human diversity of Eastern Africa is still poorly known, precluding any analysis of the
29 potential factors that shaped human diversity in the region, and more broadly throughout the
30 continent.

31 This paper describes the variation and affinities of a new group of fossil mandibles from the site of
32 Nataruk in West Turkana, Kenya, dating to ~10 Ka (Mirazón Lahr et al., 2016). In the context of a
33 scarce African fossil record, the discovery in August 2012 of this new Kenyan site is important.
34 Nataruk is located ~30 km southwest of Lake Turkana, and ~2 km from the paleoshore of Lake
35 Turkana during the AHP. The site is at the Eastern edge of a small depression that would have
36 formed a lagoon during periods of high precipitation, abutting small dunes rising ~4 m above the
37 surface. Small- to medium-sized gravel, lying loosely over a layer of lake sediments, covers the
38 surface of the ridge and mounds largely characterised by shell and carbonate deposits. The majority
39 of the fragmentary faunal remains recovered are aquatic/lake-edge species. The site has been dated
40 using radiocarbon from shells and sediment samples associated with the human remains, optical
41 luminescence dating and uranium-series dates that yielded an age estimate of ~10.5-9.5 Ka (Mirazón
42 Lahr et al., 2016). A minimum of 27 fossil individuals, among which 12 are represented by partially
43 complete skeletons, were uncovered at Nataruk. Ten skeletons show evidence of human-inflicted
44 trauma and the site was described as being the scene of inter-group conflict between hunter-fisher-

1 gatherer groups and the earliest evidence of warfare (Mirazón Lahr et al., 2016). Most of the 12
2 articulated skeletons are reasonably well-preserved; however, the crania are broken or partly
3 missing. For four specimens (KNM-WT 71258, 71259, 71260, and 71265), the skull is fragmentary;
4 another four individuals lack most of the upper face (KNM-WT 71251, 71255, 71256 and 71263),
5 KNM-WT 71253 lacks most of the occipital and basicranium, and KNM-WT 71254 preserves only the
6 right parietal, the frontal and the right zygomatic. KNM-WT 71257 and 71264 skulls are almost
7 complete, but their calvaria are deformed due to trauma. However, with the exception of KNM-WT
8 71258, 71259, 71260 and 71265, all the specimens have well-preserved mandibles that exhibit
9 minimal traumatic lesions, although most mandibular condyles are missing; the right ascending
10 ramus of KNM-WT 71254 has a linear perforation on its antero-lateral surface (see Mirazón Lahr et
11 al., 2016; Fig. 1 and 2, Table 2), but this lesion has not affected its overall shape. Therefore, while the
12 cranial remains from Nataruk are either fragmentary or show evidence of violent trauma, which
13 precludes unbiased morphometric study, the well-preserved mandibular remains offer the
14 opportunity of exploring population diversity in Africa at the height of the 'African Humid Period'.

15 In this paper we examine the phenotypic variation of the people of Nataruk in order to understand
16 their phenetic affinities with worldwide populations, and, more specifically with African populations.
17 The population affinities of the people of Nataruk have not been explored before, although our
18 expectation is that they will show a close relationship to neighbouring fisher-forager groups from the
19 early Holocene of Turkana, and more broadly, to early Holocene Eastern African forager groups.
20 While this hypothesis is based on the spatial and temporal proximity that would have promoted the
21 connectivity among these groups, the potential relationships of the Nataruk population to other
22 African populations is unmapped. Thus, this paper aims to test both this hypothesis and describe the
23 broad phenetic relationships among some Holocene African populations, both of which depend on
24 the presence of a signal of population history in mandibular morphology.

25 *The mandible as a source of evolutionary information*

26 The human cranium is often used to reconstruct morphological and phylogenetic affinities among
27 populations and species because variation in its morphology is largely explained by a model of
28 neutral evolution, i.e., the result of stochastic processes of mutation and genetic drift (Roseman and
29 Weaver, 2004; Nicholson and Harvati, 2006; Smith, 2009; von Cramon-Taubadel, 2009a; Betti et al.,
30 2010; Galland, 2013; Katz et al., 2017). However, skull morphology must still be compatible with a
31 number of different functions. These include protection of the brain and sensory organs, food
32 processing and maintenance of the respiratory airways (Daegling, 2010). As a consequence, certain
33 regions of the skull also reflect those functions and the external factors that influence them, to
34 different degrees (von Cramon-Taubadel, 2014; Noback and Harvati, 2015b;). Notably, it has been
35 suggested that the upper face – especially the nasal cavity (Noback et al., 2011; Zaidi et al., 2017) – is
36 influenced by climate, while the mandible together with general cranial shape might be more
37 influenced by diet (Harvati and Weaver, 2006; Smith, 2009; von Cramon-Taubadel, 2009b, 2011;
38 Noback and Harvati, 2015a). Nevertheless, such shape differences associated with climatic (Zaidi et
39 al., 2017) and dietary pressures (Katz et al., 2017) are relatively small, most strongly expressed at the
40 extremes of the adaptive range (i.e., among populations who live in very extreme environments),
41 and overlap between populations is considerable, indicating that the impact of these factors on skull
42 morphology may be less significant than previously hypothesised.

1 A recent study by Katz and colleagues (2017) suggests that the phenotypic differences due to diet in
2 both mandible and cranium tend to be smaller than typical differences between sexes, groups of
3 average relatedness and between individuals, further indicating that differences attributable to
4 subsistence strategy may appear somewhat magnified when comparing populations which are
5 closely related. The study, nevertheless, points towards modest directional shape differences
6 between foragers and farmers, as has been advocated before (see von Cramon-Taubadel, 2011).
7 This can be explained by a decrease in masticatory stress associated with the transition from tougher
8 or harder foraged foods to tender or soft processed agricultural ones (González-José et al., 2005;
9 Lieberman, 2008; von Cramon-Taubadel, 2011; Noback and Harvati, 2015a; Katz et al., 2017).
10 However, if the magnitude of shape difference induced by diet is relatively small, it may be assumed
11 that neutral evolution (i.e., genetic drift, gene flow reflecting population history) is the primary
12 evolutionary process by which the human cranial and mandibular phenotypic diversity has been
13 shaped (Katz et al., 2017). Therefore, while discerning between the contributions of adaptation and
14 plasticity to cranial and mandibular shape variation is complex, adult cranio-mandibular morphology
15 does record evolutionary history and can be used to track population history. Its known sensitivity to
16 environmental and lifestyle factors acting at different temporal scales, and expressed to different
17 degrees in particular morphological regions of the skull and mandible, has, nevertheless, to be taken
18 into account.

19 The present study uses mandibular morphology to assess the phenetic relationships of the Nataruk
20 population, while discussing environmental and lifestyle factors that could have influenced the
21 morphological diversity observed. We provide a complete morphological description of the eight
22 best-preserved mandibles from Nataruk, as well as an assessment of their morphological variation
23 using geometric morphometric techniques. We aim to quantify the morphological diversity observed
24 in the Nataruk mandibles to clarify their affinity to other prehistoric and historic human populations
25 both within and outside Africa.

26

27 **Materials and methods**

28 *Materials*

29 The study sample is composed of eight mandibles from Nataruk (Fig. 1 and 2, Tables 1 and 2;
30 Mirazón Lahr et al. 2016). The state of preservation of the sample is varied, but all individuals
31 included preserve the mandibular body and at least most of one of its mandibular rami. In order to
32 assess the morphological variability and affinity of the Nataruk mandibular sample, we compared
33 these specimens to a sample of 304 adult modern human mandibles. The comparative sample, listed
34 by population (Table 1) and by sites in case of fossils (Table 2) was chosen to cover a wide range of
35 chronological and spatial variation. Chronologically, the range incorporates examples from the late
36 Pleistocene (100 - 12 Ka, $n=49$), early Holocene (12 - 6 Ka, $n=14$), late Holocene (6 - 2 Ka, $n=63$) and
37 19th and 20th centuries ($n=178$); geographically, the specimens originate from sub-Saharan Africa
38 ($n=77$), North Africa ($n=101$), continental Asia ($n=12$), South Asia ($n=31$), Europe ($n=28$), Oceania
39 ($n=37$) and Greenland ($n=18$). The recent European mandibles ($n=17$) originate from England ($n=10$)
40 and from Eastern Europe ($n=7$) in order to capture more of the European morphological variation.
41 We selected a high percentage of African specimens, not only because Africa offers the best
42 comparative framework with which to understand the morphological variation of the Nataruk

1 population, but also because Africa shows the highest genetic diversity compared to other regions of
2 the world and represents a wide range of adaptive niches. Additional information on the remainder
3 of the comparative sample can be found in the Supplementary Online Material (SOM) Table S1.

4 The sample is estimated to be composed of 35.3% female and 64.7% male individuals (SOM Table
5 S1). The sex was established from previous studies; however, for almost half of the sample (i.e.,
6 47.11%), this information was lacking in the literature, and sex determination was established on the
7 secondary sexual characteristics of the skull (see Buikstra and Ubelaker, 1994; White et al., 2011).
8 The sex ratio (n females/ n total *100) for each population is indicated in Table 1.

9

10 **Table 1 and Table 2**

11

12 *Methods*

13 Morphological description The morphology of the eight Nataruk specimens is described in detail,
14 and the main morphological features of the mandibles are analysed in light of known morphologies
15 generally considered to be specific to modern humans and Neandertals.

16

17 Geometric morphometric analyses Mandibular shape was captured through 54 landmarks (six
18 medial and 24 bilateral landmarks) selected to maximise the characterisation of the mandible's
19 morphology whilst taking into consideration the state of preservation of the specimens. Missing
20 landmarks were estimated by mirroring and, where mirroring was impossible, by a thin-plate-spline
21 (i.e., TPS) interpolation using the available landmarks (Bookstein, 1989). In order to evaluate the
22 performance of TPS in estimating the missing landmarks, we simulated missing landmarks on 30
23 complete cases and tested the averages and variances of the simulated imputations (SOM, Fig. S1).
24 To correct for bilateral asymmetry in each specimen, the right and left configurations were scaled to
25 unit centroid size, before being aligned using a Generalized Procrustes Analysis (i.e., GPA, see
26 Gower, 1975; Rohlf and Slice, 1990) and rescaled to their original size. The mean coordinates, based
27 on a total of 30 landmarks per specimens (SOM Table S2, Fig. 4), were used to perform the
28 subsequent analyses on the mandibles.

29 Each landmark data set was then superimposed using a GPA, which allows for the isolation of the
30 size (i.e., centroid size) from the shape component (i.e., Procrustes residuals). The two variables can
31 be analysed independently to identify phenetic signals in the data.

32

33 Statistical analyses To explore the patterns of morphological variation within the mandibular sample,
34 and to decipher the phenetic affinities of the Nataruk mandibles, we ran three different sets of
35 analyses. Firstly, an analysis of size variation, represented by the centroid size extracted from the
36 GPA; secondly, an analysis of shape variation, represented by the Procrustes residuals and the
37 principal components obtained after between groups principal components analyses (i.e., bgPCA),
38 and finally, phenograms were built using a neighbour-joining algorithm (Saitou and Nei, 1987) based

1 on Euclidian distances calculated from shape data. All analyses were run from the same database
2 organised in different groups. First, we analysed the 23 worldwide populations of the database, we
3 then analysed 10 meta-populations which regroup some of the previous populations within
4 geochronological coherent categories, and finally, we focused on the African sample only,
5 considering both extant and prehistoric samples (Tables 1 and 2).

6 To visualize the difference in size between the groups, we built boxplots using the centroid size
7 (Table 3) extracted from the results of the GPA (Fig. 3).

8 The shape variation within the sample was explored using bgPCA based on the Procrustes residuals
9 (Fig. 4, 5 and 6, SOM Table S3). The bgPCA tests the significance of the between group distances
10 (Tables 4, 5 and 6). We used the worldwide populations, meta-populations and the African
11 populations as group variables.

12 Finally, in order to infer the biological affinity and population history of the Nataruk mandibles, we
13 built neighbour-joining phenograms (Fig. 7) using all PCs from PCAs (SOM Table S4) run on
14 population mean shapes to compute Euclidean distances. Ten thousand bootstrap replications were
15 run on the obtained phenograms in order to test for the stability of tree topology.

16 All analyses were performed on the R platform using the Morpho (version 2.1; Schlager, 2013) and
17 Geomorph (version 2.1.2; Adams and Otárola-Castillo, 2013) packages for the 3D geometric
18 morphometric analyses, the Ade4 (version 1.7-4; Dray and Dufour, 2007) package for the bgPCA, and
19 the Phangorn package (Schliep, 2011) for the neighbor-joining analyses.

20

21 **Results**

22 *Morphological description*

23 The Nataruk mandibles are large and strongly built as exemplified by their centroid size (see
24 Centroid size below), which is, on average, larger than the other meta-populations of the
25 comparative sample (Table 3). Additionally, they show wide rami and mandibular corpora (Fig. 1 and
26 2).

27

28

28 **Table 3**

29

30 On the symphyseal region, we note a strongly developed mentum osseum in most of the specimens
31 showing the characteristic modern human inverted 'T' chin (Schwartz and Tattersall, 2000). The
32 mentum osseum is slightly less salient on KNM-WT 71263 (Fig. 2C), but this may be due to the cracks
33 on the anterior surface of the symphyseal region of this specimen. It is important to note that the 3
34 females of the Nataruk sample show a strongly developed and projecting mentum osseum. The
35 alveolar region is strongly curved, with a well-marked incurvatio mandibulae, and the incisors
36 project beyond the edge of the symphysis. This feature is less developed on the KNM-WT 71251 and
37 KNM-WT 71256 fossils; however, KNM-WT 71251 is strongly distorted in this region, with the

1 incisors being compressed antero-posteriorly, and KNM-WT 71256 lacks both the crowns of the
2 incisors and some alveolar bone surrounding the missing 2nd left incisor root.

3 The upper and lower margins of the mandibular corpora diverge strongly towards the front. A
4 mandibular corpus with parallel margins is more characteristic of older hominin fossils (Mounier et
5 al., 2009). Additionally, the lower margin of the corpus displays a strongly marked inferior curvature.
6 This character seems to relate to size, with larger mandibles having a more curved lower margin (see
7 below and Figure 6). On the lateral surface of the mandibular corpus, the mental foramen is
8 positioned either at the level of the M1-P4 septum (KNM-WT 71251, 71254, 71257, 71264) or at the
9 level of the P4 (KNM-WT 71253, 71255, 71256, 71263), which is positioned slightly backwards
10 compared to most modern humans (Mounier et al., 2009). The prominentia lateralis is also
11 positioned backwards, as it is found either under M2 (KNM-WT 71256 and 71263) or even at the M2-
12 M3 level. A prominentia lateralis positioned under the third molar is often considered a Neandertal
13 apomorphy (Mounier et al., 2009); however, it is also linked to the general dimensions of a
14 specimen, and in large modern human mandibles such a morphology is not uncommon. In norma
15 lateralis, there is no retromolar space between the third molar and the ascending ramus, but we
16 note the presence of a rather large oblique retromolar surface on all the mandibles.

17 **Figure 1**

18
19 The ascending rami are relatively wide, and the projection of the anterior-most part of the ramus on
20 the mandibular corpus accounts for almost half of the mandibular total length. The deepest point of
21 the mandibular notch is generally positioned in a posterior position, which has been described as a
22 Neandertal characteristic feature in the past (Rak et al., 2002). However, this configuration of the
23 mandibular notch can be found in modern humans, and as is the case with the prominentia lateralis,
24 it also seems to be related to the general size of the specimen (Mounier et al., 2009). The condyle
25 and coronoid process are equally elevated in most specimens, with the exception of KNM-WT 71253
26 and 71254, in which the condyle is slightly higher than the coronoid process. The mandibular notch
27 joins the condyle in a lateral position, as is usually the case in modern humans. The gonial angle is
28 regular and strongly everted in almost all specimens (with the exception of KNM-WT 71254 and
29 71255 which are both females), indicating strong muscle attachments.

30 The medial aspect of the mandible, unsurprisingly, does not display a planum alveolare. The
31 mylohyoid line is well marked and usually inclined, with the exception of KNM-WT 71257 in which it
32 is more diagonally orientated, a character that recalls the Neandertal morphology (Rosas, 1992;
33 Creed-Miles et al., 1996). The mylohyoid line is positioned relatively low at the M3 level, except for
34 KNM-WT 71251 and 71255; again, although this trait is observed in modern human mandibles
35 (Mounier et al., 2009), it has been argued to be more common among Neandertals (Rosas, 1992;
36 Creed-Miles et al., 1996).

37 In sum, the Nataruk mandibles, while having a very clear modern human morphological pattern,
38 show a number of features that are common in other hominin species, such as the Neandertals.
39 Such a phenotypic pattern has been described before in other early Holocene African populations,
40 for instance the specimens from Assie-el-Habiod in Northern Mali (Dutour, 1989; Mounier et al.,
41 2009) and Iwo Eleru in Nigeria (Harvati et al., 2011). However, most of the archaic morphological

1 traits may be linked to size, which, in the case of Nataruk, is not surprising considering the large
2 dimensions (see Centroid size below) of the fossils.

3

4

Figure 2

5

6 *Centroid size*

7 A comparatively large average centroid size is one of the distinguishing features of the Nataruk
8 mandibles. Here we compare the differences in centroid size between the populations and meta-
9 populations of our sample (Table 3).

10 Figure 3 shows the distribution of the centroid size for each specimen according to their worldwide
11 populations, meta-populations and within the African sample only. First, we note that the extant and
12 pre-Dynastic populations are generally smaller than the early Holocene and Pleistocene specimens.
13 The extant and pre-Dynastic specimens appear to have similar size with the exception of the gracile
14 sub-Saharan Khoisan, the South-East Asian Andamanese Negritos, and, to a lesser extent, the pre-
15 Dynastic Badari which are the smallest populations of our sample (Figure 3A). Figure 3B shows that,
16 when considered as meta-populations, there is virtually no size difference between the pre-Dynastic
17 and recent populations. On the contrary, the Nataruk mandibles are in the higher range of size
18 variation of our comparative sample in both cases. Their size is only matched by the late Pleistocene
19 fossils from North Africa (Afalou and Taforalt) and by the North African fossil Nazlet Khater 2. Most
20 of the Holocene fossils from the Central Rift Valley (i.e., Elmenteita A, D and F1, Gamble's Cave 4 and
21 5, Nakuru IX and Wiley Kopje II) and the European Pleistocene specimens (i.e., Dolní Věstonice 3, XIII,
22 XV, Pavlov I, Předmostí 4 and 3, Abri Pataud 1, Chancelade, Kostenski 14, Oberkassel 2) tend to be
23 smaller than the North African fossils and Nataruk; they fit within the range of variation of the extant
24 human sample. Finally, the mandibles from Lothagam appear to be slightly bigger than the Nataruk
25 specimens, and the largest of the comparative sample. When looking at Figure 3C, we note that all
26 of the Central Rift Holocene specimens, except one mandible from Elmenteita, are within the extant
27 range of size variation while, again, the Nataruk specimens, along with Lothagam and the North
28 African Pleistocene fossils, are larger.

29

30

Figure 3

31

32 *Shape variation – between groups PCA*

33 Figure 4 shows the first two bgPCs (56.58% of the total variance, SOM Table S3) of the bgPCA based
34 on the Procrustes residuals of the analysis of the individual specimens grouped according to the 23
35 worldwide populations. Along bgPC1 (29.78% of the total variance) the shape deformation in the
36 negative values represents a mandible with a strongly developed incurvatio mandibulae and
37 mentum osseum, a deep mandibular body with margins that are strongly converging backwards, and
38 a vertical wide and short ramus. On the positive side of the axis, the mandibular corpus is low with

1 almost parallel margins, and the ramus is narrow and tall, making a wide open angle with the corpus.
2 Additionally, the general length of the mandible increases along bgPC1. Along the second
3 component (26.80% of the variance), the mandibular corpus and the mandibular ramus become
4 thinner and more elongated; additionally, the general width of the mandible increases.

5

6

Figure 4

7

8 The dispersion of the cloud of points within the morphospace shows little separation among the
9 comparative populations. We can, however, see that the Asian populations along with the Inuit,
10 Papuan and, to a lesser extent, Australian specimens tend to share the morphospace represented by
11 positive bgPC1 values; the Africans and Europeans are mainly positioned at the centre of bgPC1,
12 while the chronologically older samples (Afalou, Taforalt, Nazlet Khater 2, Holocene Central Rift and
13 Lothagam) present negative values on bgPC1. It is worth noting that the Pleistocene specimens from
14 Europe do not follow this pattern as they group at the centre of the chart with extant populations.
15 Most populations are not discriminated along bgPC2, with the exception of the North African
16 Pleistocene specimens (Afalou and Taforalt) from Nataruk and Lothagam samples. In more detail,
17 the Nataruk specimens (black) are positioned at the margin of the main cloud of points, along with
18 the Early Holocene specimens (red) from Lothagam and, to a lesser extent, from the Central Rift.
19 This last group displays, nevertheless, a much wider variation, as exemplified by the 90% confidence
20 interval ellipse of the group which extends into the central part of the morphospace. The
21 permutation test results run on the bgPCs (Table 4) indicate that, despite the overlap of most of the
22 populations within the morphospace, the pairwise group differences are, in most cases, significant.
23 The Nataruk specimens cannot be distinguished from Lothagam, the Holocene Central Rift
24 specimens and from the Nazlet Khater 2 isolated fossil. Their morphology appears different from
25 that of the other populations considered.

26

27

Table 4

28

29 The second bgPCA was run between meta-populations, regrouping different populations into larger
30 coherent geo-chronological groups. The first two bgPCs displayed in Figure 5 represent 67.97% of
31 the total variance of the shape data (bgPC1: 39.68%; bgPC2: 28.29%). The mandibular shapes
32 described are very similar to those of the first bgPCA, with reverse polarity along bgPC1, and an
33 added general decrease in length of the mandible from negative to positive values, with mandibular
34 corpus margins that become more parallel along bgPC2.

35

36

Figure 5

37

1 The morphospace (Fig. 5) displays a good separation between the means of each extant meta-
2 population. BgPC1 separates individuals from Oceania and Asia from Africans and Europeans, while
3 bgPC2 sets apart Europe, Asia and the North African Nile Valley specimens. Only the Inuit and sub-
4 Saharan mandibles cannot be separated within the morphospace. The African early Holocene and
5 Pleistocene samples present positive values on the first component, hence, occupying a different
6 morphospace from the rest of the sample. This is not the case of the European Pleistocene
7 specimens, which group around the Inuit and extant sub-Saharan African mandibles at the centre of
8 the chart. It is worth noting the difference in shape between extant and Pleistocene Europeans, the
9 prehistoric sample being more similar to extant sub-Saharan African and Inuit specimens than to
10 current Europeans. The second component separates Nataruk and most of the early Holocene
11 Kenyan specimens from the North African Pleistocene fossils. Looking at the permutation test results
12 (Table 5) confirms these visual observations, as Nataruk and the early Holocene specimens from
13 Kenya are the only groups which are not statistically different.

14

15

Table 5

16

17 The last bgPCA was run on the African populations only. Figure 6 presents the two first bgPCs,
18 representing 61.84% of the variance. Along the first component (36.09% of the total variance) the
19 general length of the mandible decreases from negative to positive values, the mandibular ramus
20 becomes thinner and more elongated and the mentum osseum becomes more strongly developed
21 along with the incurvatio mandibulae. The shape deformation associated with bgPC2 (25.75% of the
22 variance) in the positive values represents a mandible with a deep mandibular body, the margins of
23 which are strongly converging backwards, and a vertical ramus; on the negative side of the axis, the
24 mandibular corpus is low with almost parallel margins, and the ramus is narrow, making a wide open
25 angle with the corpus.

26

27

Figure 6

28

29 The morphospace (Fig. 6) separates on bgPC2, extant and pre-Dynastic Nile Valley populations from
30 the Pleistocene and early Holocene ones, with the notable exception of Nakuru IX and one of the
31 Gamble's Cave mandibles, which are positioned within the point clouds of recent Africans. On
32 bgPC1, the sub-Saharan populations are separated from the Naqada and Kerma pre-Dynastic groups,
33 while Badari and Jebel Moya appear to be more similar to the Somali, Bantu and Haya specimens.
34 Regarding the Nataruk fossils, once again they are very similar to the mandibles from Lothagam, and
35 to some of the Central Rift Valley fossils from Elmenteita and Gamble's Cave. It is worth noting that
36 the shape of Willey Kopje II is closer to the North-African Pleistocene populations from Afalou and
37 Tforalt than to the other early Holocene East African mandibles. The pairwise comparison of the
38 group differences (Table 6) indicates first that groups with a low number of individuals (i.e.,
39 Gamble's Cave, Elmenteita, Nakuru, Willey Kopje and Nazlet Khater) cannot be assessed accurately,
40 as they tend to show no significant differences to any of the other populations. Second, that the

1 other populations can be generally distinguished, although the sub-Saharan groups are similar to
2 each other, with the exception of the Khoisan. Finally, that the Nataruk mandibles are once again
3 indistinguishable from those from Lothagam.

4

5

Table 6

6

7 *Phenetic affinities of the Nataruk specimens – phenograms*

8 Finally, to assess the phenotypic affinity of the Nataruk specimens, we analysed the mean shape of
9 each population through PCAs and Neighbour-Joining trees based on the Euclidian distances with a
10 10,000 replication bootstrap. We performed this analysis separately on the 23 worldwide
11 populations (Fig. 7A), the 10 meta-populations (Fig. 7B) and on the African populations only (Fig. 7C).

12 Figure 7A depicts the pattern of affinity between the 23 worldwide populations. On the left, the plot
13 of the first two PCs from the PCA (56.23% of the variance) clearly shows the relatively unusual shape
14 of the mandibles from Nataruk and Lothagam, which are similar only to the Pleistocene North-
15 African Nazlet Khater 2 specimen. Most sub-Saharan African populations tend to cluster around the
16 centre of the chart, while some Nile Valley groups and Eurasians occupy the lower left part of the
17 morphospace. It is worth noting the apparent affinity in mandibular shape between the Inuits and
18 some sub-Saharan populations (Haya and Bantu) and with the Pleistocene European fossils. The late
19 Pleistocene North African fossils from Afalou and Taforalt occupy a central bottom position in the
20 morphospace, along with the early Holocene Central Rift specimens, the shapes of which are,
21 nevertheless, less extreme. On the right, the unrooted phenogram appears divided into two main
22 clusters. The upper part of the tree contains recent human populations, with the exception of the
23 samples from Badari and Jebel Moya, and of Pleistocene European fossils, which cluster loosely with
24 the Khoisan (18% of 10,000 bootstrap replications) and the Inuits (9%). sub-Saharan (Somali, Bantu
25 and Haya) and Nile Valley (Badari and Jebel Moya) populations cluster on both sides of this group.
26 The rest of this cluster is composed of South-East Asian and Oceanian populations, with a strong
27 association of Australians and Andamans (42%) on the one hand, and of Papuans and Nicobarese
28 (36%) on the other. The second main cluster is composed mainly of early Holocene or Pleistocene
29 African specimens, as well as extant Eurasian mandibles. The North African samples from Afalou and
30 Taforalt cluster together (43%), before grouping with a cluster that includes, sequentially, two Nile
31 Valley populations, Naqada (27%) and Kerma (26%), and China and Europe (33%), which are closely
32 associated (62%). Finally, the rest of the cluster is composed of the early Holocene Kenyan
33 populations (Lothagam and Holocene Central Rift) and the North African Pleistocene mandible from
34 Nazlet Khater, which are grouped around the Nataruk fossils. Nataruk is strongly associated with
35 Nazlet Khater 2 (62%) and Lothagam (26%).

36

37

Figure 7

38

1 Figure 7B, which depicts the results based on the 10 meta-populations, shows a clearer phenetic
2 signal. The morphospace defined by the first two PCs (67.85% of the variance) is divided between
3 groups with PC1 values ≥ 0 and PC2 values ≤ 0 (Pleistocene North Africa, Holocene Kenya and
4 Nataruk) and the opposite (all extant worldwide populations, as well as, again, the Pleistocene
5 Europeans). Oceania, Asia and Europe tend to show an extreme of mandibular variation along PC1
6 (left of the morphospace), while extant sub-Saharan African, Inuit and, to a lesser extent, Nile Valley
7 and Pleistocene European samples occupy a more central position. Pleistocene Europe and
8 Pleistocene North Africa occupy opposite extremes along PC2. The unrooted tree on the right
9 highlights a coherent phenetic pattern. The upper part of the tree shows the relationships between
10 extant populations, with the sub-Saharan meta-population clustering (19%) with a group formed by
11 Oceania and Asia (29%) and Europe and the North African Nile Valley (5%); the Inuit cluster with the
12 Pleistocene Europeans (40%). The lower part of the phenogram is composed of the Pleistocene
13 North Africans grouped with Nataruk (44%) and the other early Holocene East Africans (65%).

14

15 Finally, the last analysis concerns the African populations only, and allows us to compare Nataruk to
16 individual sites from the Holocene Central Rift Valley of Kenya (Gamble's Cave and Elmenteita and
17 the Neolithic sites of Willey Kopje and Nakuru). The morphospace depicted on Figure 7C represents
18 56.48% of the variance and indicates that recent African populations, along with Jebel Moya and the
19 pre-Dynastic Badari, share a common morphospace in the bottom centre of the chart. The other
20 populations are more dispersed, and the oldest specimens tend to occupy the top of the
21 morphospace. It is worth noting that Nakuru IX shows an extreme morphology which is nevertheless
22 persistently closer to the Maghrebian fossils from Afalou and Taforalt than to any other sample or
23 individual in the dataset, while Nataruk, Lothagam and Nazlet Khater share a common shape
24 pattern. The unrooted phenogram (Fig. 7C, right) has two main branches. The first one is composed
25 of recent sub-Saharan Africans (40%) grouped together with the prehistoric population from Sudan,
26 Jebel Moya, and the pre-Dynastic Egyptians from Badari (22%), with two strongly supported clusters:
27 Bantu-Haya (69%) and Khoisan-Jebel Moya (48%). The second branch supports two groups: a mostly
28 Northern African one, with two Nile Valley populations (Naqada and Kerma, 48%) and the late
29 Pleistocene fossils from Taforalt and Afalou (28%), and which includes the East African Nakuru IX
30 specimen (48%); and a mostly East African one, which clusters all the other Central Rift Valley fossils
31 (with a branch linking the fossils from Gamble's Cave and Willey Kopje II, 44%), along with a branch
32 that includes the Elmenteita samples (45%) and a sub-cluster that groups the Nataruk-Lothagam
33 mandibles (30%), with the Egyptian fossil from Nazlet Khater (64%).

34 In sum, while not all the resulting population clusters follow coherent affinity patterns, we note that
35 some groupings reflect aspects of population history: the populations from Oceania with South
36 Asians (Sri Lanka, Nicobar Is. and Andaman Is.), a mainland Eurasian grouping of Chinese and
37 European populations, and most of the sub-Saharan groups which cluster tightly together.
38 Additionally, the analyses highlight the diversity among the prehistoric Nile Valley populations, with
39 two (Naqada and Kerma) recurrently associated with the late Pleistocene specimens from Afalou
40 and Taforalt, as well as with the early Holocene Central Rift fossils, and the other two (Badari and
41 Jebel Moya) more similar to extant sub-Saharan populations. Considering the phenotypic affinity of
42 the Nataruk sample within both a worldwide and an African context, the analyses highlight the
43 strong affinities that exist between Nataruk and other early Holocene populations from East Africa

1 (i.e., Lothagam, Gamble's Cave and Elmenteita). They also show strong relationships with
2 Pleistocene specimens from North Africa, Afalou and Taforalt and, more surprisingly, with the much
3 older Nazlet Khater 2 specimen. These results place Nataruk within an East African, fisher-hunter-
4 gatherer morphological continuum in the early Holocene, which shares strong affinities with late
5 Pleistocene fossils from Northern Africa.

6

7 **Discussion**

8 This study of the mandibles from the site of Nataruk brings new information on the morphological
9 variation of early Holocene populations from Eastern Africa. While previous studies have stressed
10 the role of diet in shaping mandibular morphology (Lieberman, 2008; von Cramon-Taubadel, 2009b),
11 recent evidence has weakened this interpretation (Katz et al., 2017). Both von Cramon-Taubadel
12 (2009b) and Katz et al. (2017) conclude that the shape of the mandible does reflect subsistence
13 strategy. However, von Cramon-Taubadel (2009b) suggests that this effect is very significant, to the
14 extent that it erases the signature of past populations' history, Katz and colleagues (2017) have
15 shown that mandibular phenotypic variation is mostly due to individual variation, which, when
16 examined at a population level, shows that the impact of diet is dwarfed by neutral evolutionary
17 processes. Results from the present study tend to support the second hypothesis, as without
18 considering any environmental factors in the phenetic analyses of our mandibular sample, our
19 results provide a clear recurrent phenetic and/or population history signal.

20 For instance, when looking at the size of the mandible of different populations, we note that
21 populations representing different environments and dietary adaptations, such as Australians and
22 Inuit (hunter-gatherers), and Europeans and Papuans (farmers/horticulturalists), cannot be
23 distinguished in terms of centroid size (Fig. 3A). In fact, between group centroid size variation in our
24 sample is surprisingly low when considering extant human populations (Fig. 3A and B), with the
25 exception of the Andaman Islanders, a group of Negritos from Southeast Asia. The small mandibular
26 size of the latter is part of their distinctive overall small body size, reflected in a mean adult stature
27 for males of ca. 148 cm (Stock and Migliano, 2009). Only the early Holocene and late Pleistocene
28 fossils tend to be larger, and, in that respect, the Nataruk sample centroid size is within the expected
29 variation from an early Holocene fisher-gatherer population from East-Africa (Fig. 3).

30 In terms of the shape of the mandible of extant human populations, subsistence strategy does not
31 seem to have a major impact on the results obtained. For instance, the results from the first bgPCA
32 (Fig. 4) show that some of the hunter-gatherer groups (Australians and Andamanese) are not
33 particularly separated from farmer/horticulturalist populations: the Andamanese are similar to the
34 geographically close specimens from the Nicobar Islands, and Australians share similarities with the
35 Nile Valley populations from the sites of Naqada and Kerma. The Neighbour-Joining analysis (Fig. 7A)
36 shows a somewhat more ambiguous signal, as we note the clustering of the Australians with the
37 Andamanese along with the clustering of Papuans with Nicobar Islanders. This pattern of similarities
38 between hunter-gatherer on the one hand and farmer/horticulturalist on the other goes against
39 genomic data which indicates a strong phylogenetic relationship between Australians and Papuans
40 (Malaspinas et al., 2016). They, nevertheless, cluster into two closely related groups, which fall
41 within a larger South-East Asia-Oceania cluster (i.e., Sri Lanka, Australia, Andaman, Papuan and
42 Nicobar, see Fig. 7A). This association could depict the complex phenetic links between those

1 populations that may reflect the differential retention of an ancient signature of dispersal (Lahr and
2 Foley, 1994; Lahr, 1996; Reyes-Centeno et al., 2014; Pagani et al., 2016), the hypothesis of a deep
3 genetic divergence of these groups from other South Asian populations (Bergström et al., 2016), and
4 the shared pattern of archaic genomic admixture (Malaspinas et al., 2016; Mondal et al.; 2016)). The
5 influence of population of origin in shaping the mandibular phenotype is also exemplified by some
6 well-described phenetic patterns in the Neighbour-Joining trees (Fig. 7). For instance, in the
7 worldwide population analysis, besides the clustering of the populations from Oceania and South
8 Asia, the Chinese and Europeans are closely associated, a result that is also coherent with recent
9 genomic studies (Mallick et al., 2016; Pagani et al., 2016).

10 The shape analyses also show that all the specimens older than 5,000 years BP (i.e., early Holocene
11 and Pleistocene) occupy the same sector of the morphospace defined by the first 2 PCs of the PCAs
12 run on the mean shape of the different populations (Fig. 7), the only exception being the Pleistocene
13 European sample, which tends to share affinities with the Inuit and recent Sub-Saharan (especially
14 Khoisan) populations (Fig. 7A and B). Such an association between geographically and/or
15 chronologically distant hunter-gatherer groups (Pleistocene Europe, Khoisan and Inuit), may
16 nevertheless not be indicative of a functional response of mandibular morphology to their shared
17 subsistence strategy, since morphological and ancient genomic results suggest that both the South
18 African Khoisan and the Inuit may preserve signatures of complex ancestral relationships with
19 Pleistocene Europeans (Grine et al., 2007; Raghavan et al., 2014; Flegontov et al., 2016; Schlebusch
20 et al., 2017). Some of the prehistoric populations of the Nile Valley (Naqada and Kerma) show strong
21 similarities with the late Pleistocene North African fossils from Afalou and Taforalt (Fig. 7A and C).
22 This affinity seems to represent phylogenetic proximity, as those populations lived in different
23 environments and did not share a common subsistence strategy: Afalou and Taforalt were hunter-
24 gatherers (Aoudia-Chouakri, 2013) while Naqada and Kerma were early farmers (Simon, 1989;
25 Hendrickx, 1999). However, the other Nile Valley populations cluster differently: Jebel Moya and
26 Badari show similarities with sub-Saharan African samples (Khoisan, Somali, Haya and Bantu). This
27 latter pattern is recurrent, and may be partly explained by the complexity of the site of Jebel Moya.
28 The site, which includes three occupation phases (Gerharz, 1994; Brass and Schwenniger, 2013), lies
29 at the boundary between North and sub-Saharan African geographic spheres (Brass, 2014) and may
30 preserve an admixed population exhibiting a mosaic of features that are reminiscent of both sub-
31 Saharan and North African peoples (Irish and Konigsberg, 2007). The sub-Saharan affinities of the
32 early pre-Dynastic population from the Egyptian site of Badari observed recurrently in our analyses
33 should be investigated further. The best evidence that mandibular morphology captures phenetic
34 relations is the close association between the Nataruk and Lothagam mandibles observed in every
35 analysis performed. These two samples originate from sites that are spatially and temporally close,
36 and probably represent sub-groups from a single population of fisher-foragers of Southwest Turkana
37 during the early phase of the African Humid Period. Mandibular morphology captures the underlying
38 phenetic signal that describes this close relationship.

39 As a whole, our morphometric data provide a phenotypic signal that can be interpreted clearly in a
40 phenetic framework.

41

42 *Who were the Nataruk people? – Phenetic affinity of the mandibles from Nataruk*

1 The results from this study recurrently show that the Nataruk mandibles share their strongest
2 affinities with the Lothagam specimens as hypothesised: they are similar in size (Fig. 3A and C) and
3 similar in shape, as illustrated by both the bgPCAs results (Fig. 3, 4 and 5) and by their mean
4 Procrustes distance and position in the Neighbour-Joining trees (Fig. 7A and C). This affinity is
5 expected, since the two sites are in close geographical proximity (about 25 km apart) and of overall
6 similar age (Robbins, 1974; Mirazón Lahr et al., 2016), and could represent sub-groups from the
7 same population. The second expectation, that the Nataruk mandibles would share shape affinities
8 with early Holocene specimens from East Africa, here represented by a sample from the Central Rift
9 Valley, is also met, as exemplified by the clustering of most of the Central Rift specimens with
10 Nataruk in all three Neighbour-Joining trees (Fig. 7). Those affinities are supported by strong
11 bootstrap values which underline the likely phylogenetic links between Eastern African populations
12 dated between 10,000 and 6,000 thousands years BP. Nakuru IX is the only one of the Holocene
13 Central Rift Valley specimens not to cluster around the Nataruk sample. This morphological
14 difference may be explained by different factors. First, being a single specimen, we are aware that its
15 morphology may not adequately reflect the phenotype of its population of origin, and that the
16 Nakuru IX mandible may represent an extreme of the morphological variation of its people. Second,
17 the site of Nakuru is younger (Neolithic) than most of the early Holocene sample of the study;
18 however, another Neolithic specimen from the same area, Willey Kopje II, does cluster around
19 Nataruk along with the other Holocene Central Rift Valley specimens (Fig. 7C), suggesting that age
20 and subsistence is not what pulls the fossil of Nakuru IX apart from other Holocene East Africans.
21 Instead, Nakuru IX persistently shares strong affinities with the North African late Pleistocene fossils
22 from Taforalt and Afalou (15,000 to 11,000 years BP), which, as observed in the worldwide analysis,
23 also cluster with the Nile Valley North African fossils from Naqada and Kerma. Similarly, the much
24 older (36,000 years BP) Nile Valley fossil from Nazlet Khater clusters with the early Holocene Eastern
25 African specimens, suggesting an ancient connection between East Africa and the Nile Valley.

26 It is interesting to note that the third Neighbour-Joining tree including only African specimens (Fig.
27 7C) depicts clearly three different branches, each associated with a set of older populations – (1)
28 extant sub-Sahara Africans, including the pre-Dynastic Badari, and the Nubian Jebel Moya; (2) early
29 Holocene Eastern Africans (including Nataruk) and the fossil from Nazlet Khater 2; and (3) a similar
30 diachronic and geographically dispersed association among late Pleistocene groups from the
31 Maghreb (Afalou and Taforalt), the pre-Dynastic and Nubian samples from Naqada and Kerma from
32 the Nile Valley, and the Neolithic fossil (Nakuru IX) from the Central Rift Valley of Kenya as observed
33 above. The last two clusters seem to share more affinities between themselves than with the extant
34 sub-Saharan Africans.

35 In sum, the Nataruk mandibles are part of a continuum of morphological variation that links
36 Pleistocene and Holocene populations from Eastern and Northern Africa (Maghreb, Nile Valley and
37 the Kenyan Rift Valley) to the almost complete exclusion of the recent African sample.

38 Such a pattern can be interpreted first through the global climatic change that impacted the world at
39 the end of the Pleistocene. The last deglaciation, which started in the Northern Hemisphere around
40 19,000 years ago and in the Southern hemisphere around 15,000 years ago, led to two abrupt rises
41 in sea level (Clark et al., 2009), leading to the onset of an interglacial period worldwide and, in the
42 case of Africa, to a period of greatly increased precipitation known as the African Humid Period
43 (deMenocal et al., 2000). In this framework, the greening of the Sahara (Larrasoña et al., 2013) may

1 have allowed hunting–fishing populations to spread from the Northern Kenyan lakes to the Nile and
2 across the Sahel into North Africa (Mirazón Lahr, 2016). The African Humid Period lasted until
3 around 5,000 years ago (de Menocal, 2015), presumably creating multiple opportunities of increased
4 population connectivity between Eastern and Northern Africa for 10,000 years. It is of interest to
5 note that most of the populations representing North Africa in our sample date to within this time
6 span, when aquatic corridors would have allowed some connection and, presumably, gene-flow: the
7 specimens from Afalou and Taforalt, which are dated between 15,000 and 11,000 years BP (Aoudia-
8 Chouakri, 2013), and the specimens from Naqada, Badari and Jebel Moya, who lived in the Nile
9 Valley from 6,000 to 5,000 years ago (Gerharz, 1994; Hendrickx, 1999). Only the Kerma specimens,
10 dated to around 3,500 years BP (Simon, 1989), and the Nazlet Khater 2 fossil dated to 36,000 years
11 BP (Crevecoeur, 2006), are outside of the temporal span in which this North-East African connection
12 would have existed, although they may reflect both lagged patterns of survivorship/affinity (Kerma)
13 and biogeographically recurrent connections (Nazlet Khater).

14 Additionally, the site of Nataruk is located at the edge of a large paleolake (Turkana). The lithic
15 assemblage that was uncovered at the site is similar to other Later Stone Age assemblages in that
16 area (Robbins, 2006; Beyin, 2011), including fragments of barbed bone harpoons typical of early
17 Holocene fisher-foragers of Turkana (Robbins, 1975). As a result, the Nataruk people have been
18 described as representing a hunter-fisher-gatherer population (Mirazón Lahr et al., 2016). Within the
19 comparative sample of the present study, other populations present similar characteristics in terms
20 of chronology and lifestyle: the Lothagam sample, which originates from a site that is also situated at
21 the edge of Lake Turkana and is dated to a similar period (Robbins, 1974), and the Central Rift Valley
22 specimens that originate from populations that lived in the Nakuru-Elmenteita Basin between 8,000
23 and 6,000 years BP. Although Nakuru and Elmenteita are two different lakes nowadays, they formed
24 a much larger paleolake during the early Holocene (Dühnforth et al., 2006), which may have also
25 supported a fisher-forager subsistence strategy during the African Humid Period, consistent with the
26 presence of a bone harpoon at the site of Gamble’s Cave (Oakley, 1961). Although more complete
27 information concerning the life-style of the hunter-gatherers who lived in the other sites of the area
28 at the time, such as Elmenteita (Leakey, 1970), is wanting, the geographic, ecological and
29 chronostratigraphic position of the populations living at the edge of the Nakuru-Elmenteita
30 paleolake in the early Holocene suggest that they may have experienced similar conditions and may
31 have shown similar adaptive responses to the Nataruk-Lothagam population, as well as possibly
32 shared ancestry. Lastly, the Afalou and Taforalt North African groups lived near the Mediterranean
33 coast and have also been described as hunter-fisher-gatherers (Aoudia-Chouakri, 2013); their
34 relationship to AHP Saharan and Nile Valley populations remains to be fully explored.

35 Finally, it is interesting to note that neither the late Pleistocene North African sample, nor the early
36 Holocene Eastern African specimens, including the Nataruk fossils, show strong affinities to the
37 specimens representing the extant African populations in our sample. As it has been pointed out in
38 the morphological description of other late Pleistocene/early Holocene African fossils (Harvati et al.,
39 2011; Tryon et al., 2015; Crevecoeur et al., 2016), these specimens tend to exhibit distinctive
40 characteristics and higher phenotypic diversity than do extant African populations, to the extent that
41 they show more affinities with Middle to early late Pleistocene fossils (Crevecoeur et al., 2016). Such
42 a phenotypic pattern may explain the affinity shared by the Nataruk fossils and the late Pleistocene
43 fossil from Nazlet Khater 2 in our analyses, and highlights the role of an early Holocene Filter in
44 shaping current patterns of human diversity, particularly in Africa (Mirazon Lahr, 2016).

1

2 **Conclusion**

3 This study attempts to establish the phenetic affinities of the people of Nataruk, a hunter-fisher-
4 gatherer population from the early Holocene of West Turkana (Kenya), on the basis of their
5 mandibular morphology. Our findings resonate with previously observed patterns of phenotypic
6 plasticity in the human mandible, the morphology of which reflects, in part, recent adaptations to
7 environmental and behavioural factors. However, the main signal in our analyses is one that appears
8 to reflect population history. In the case of the people who were killed at Nataruk, we show their
9 strong affinities with other early Holocene hunter-fisher-gatherer populations from West Turkana in
10 particular, and Eastern Africa more generally, but also, and more surprisingly, the apparent phenetic
11 connection that may have existed between these Eastern African populations and some Nile Valley
12 and Maghrebian groups which lived at a time when a Green Sahara may have allowed substantial
13 contact, and potential gene flow, across a vast expanse of Northern and Eastern Africa. It is possible
14 that the shared aquatic fisher-forager strategies of populations who lived geographically separated
15 by the Sahara could have led to a common adaptive response that is reflected in the shape of the
16 mandible, thus convergently accounting for the strong affinities observed in the data. However, such
17 overriding functional convergence is not supported by the results of the worldwide analyses that
18 recurrently cluster groups of different subsistence strategy, nor with the totality of the observed
19 phenotypic pattern among the early Holocene African samples. This is further stressed by the fact
20 that this morphological association is not exclusive to AHP fisher-foragers, but also includes
21 populations in both the Nile Valley and Kenyan Central Rift Valley who practised a pastoralist and/or
22 agriculturalist subsistence strategy around the end of the African Humid Period. Given the limited
23 number of late Pleistocene/early Holocene African fossils available and the poor understanding of
24 the archaeological context of some of the Central Rift Valley specimens, further research is needed
25 to bring additional insight into the history of early African populations.

26

27 **Acknowledgements**

28 This study was funded by an Advanced ERC Award (IN-AFRICA Project, grant number: 295907). For
29 permission to carry out field and museum research in Kenya, we thank the Office of the President of
30 Kenya, the Turkana County government, the National Museums of Kenya, and the people of
31 Turkana. For permission to study specimens in their care, we thank directors and curators of the
32 following institutions: Musée de l'Homme (Paris, France); Institut de Paléontologie Humaine (Paris,
33 France); National Museums of Kenya (Nairobi, Kenya); Anthropos Institute (Brno, Czech Republic),
34 Open Scan Research Archive (University of Pennsylvania Museum of Archaeology and Anthropology,
35 USA), and Duckworth Laboratory (Cambridge, UK). We thank F. Lahr for assistance with CT-scanning,
36 Isabelle Crevecoeur, Patrick Semal and Stéphane Louryan for providing access to the CT-scan of
37 Nazlet Khater 2, and Todd Rae, Janet Monge and Thomas Schoenemann for helping with the ORSA
38 database. We thank F. Détroit, M. Galland and J. Corny for help and ideas. Finally, we thank M.
39 Plavcan, the Associate Editor, and two anonymous reviewers for valuable comments and criticisms
40 of earlier drafts that contributed to the improvement of this study.

41

1 References

- 2
- 3 Alarcón, J.A., Bastir, M., Rosas, A., 2016. Variation of mandibular sexual dimorphism across human facial
4 patterns. *HOMO* 67, 188-202.
- 5 Aoudia-Chouakri, L., 2013. Pratiques funéraires complexes: réévaluation archéo-anthropologique des
6 contextes Ibéromaurusiens et Capsiens (paléolithique supérieur et épipaléolithique, Afrique du nord-ouest).
7 Ph.D. Dissertation, Université de Bordeaux 1.
- 8 Bergström, A., Nagle, N., Chen, Y., McCarthy, S., Pollard, M.O., Ayub, Q., Wilcox, S., Wilcox, L., van Oorschot,
9 R.A.H., McAllister, P., Williams, L., Xue, Y., Mitchell, R.J., Tyler-Smith, C., 2016. Deep roots for Aboriginal
10 Australian Y chromosomes. *Current Biology* 25, 809-813.
- 11 Betti, L., Balloux, F., Hanihara, T., Manica, A., 2010. The relative role of drift and selection in shaping the
12 human skull. *American Journal of Physical Anthropology* 141, 76-82.
- 13 Beyin, A., 2011. Recent archaeological survey and excavation around the Greater Kalokol Area, west side of
14 Lake Turkana: Preliminary findings. *Nyame Akuma* 75, 40-50.
- 15 Bookstein, F.L., 1989. Principal warps: thin-plate splines and the decomposition of deformations. *IEEE TPAMI*
16 11, 567-585.
- 17 Brass, M., 2014. The southern frontier of the Meroitic state: The view from Jebel Moya. *African Archaeological*
18 *Review*. 31, 425-445.
- 19 Brass, M., Schwenniger, J.-L., 2013. Jebel Moya (Sudan): new dates from a mortuary complex at the southern
20 Meroitic frontier. *Azania* 48, 455-472.
- 21 Bricker, H., Mellars, P., 1987. Datations 14C de l'Abri Pataud (Les Eyzies, Dordogne) par le procédé
22 "accélérateur-spectromètre de masse". *L'Anthropologie* 91, 227-234.
- 23 Buikstra, J.E., Ubelaker, D.H., 1994. Standards for data collection from human skeletal remains. *Arkansas*
24 *Archeological Survey*, Fayetteville, AK.
- 25 Carolin, S.A., Cobb, K.M., Adkins, J.F., Clark, B., Conroy, J.L., Lejau, S., Malang, J., Tuen, A.A., 2013. Varied
26 response of western Pacific hydrology to climate forcings over the last glacial period. *Science* 340, 1564-1566.
- 27 Clark, P.U., Dyke, A.S., Shakun, J.D., Carlson, A.E., Clark, J., Wohlfarth, B., Mitrovica, J.X., Hostetler, S.W.,
28 McCabe, A.M., 2009. The Last Glacial Maximum. *Science* 325, 710-714.
- 29 Collett, M., 1933. A study of twelfth and thirteenth dynasty skulls from Kerma (Nubia). *Biometrika* 25, 254-284.
- 30 Creed-Miles, M., Rosas, A., Kruszynski, R., 1996. Issues in the identification of Neandertal derivative traits at
31 early post-natal stages. *Journal of Human Evolution* 30, 147-153.
- 32 Crevecoeur, I., 2006. Etude anthropologique des restes humains de Nazlet Khater (Paléolithique supérieur,
33 Egypte). Ph.D. Dissertation, Université de Bordeaux 1.
- 34 Crevecoeur, I., Brooks, A., Ribot, I., Cornelissen, E., Semal, P., 2016. Late Stone Age human remains from
35 Ishango (Democratic Republic of Congo): New insights on Late Pleistocene modern human diversity in Africa.
36 *Journal of Human Evolution* 96, 35-57.
- 37 Day, M., 1969. Omo human skeletal remains. *Nature* 222, 1135-1138.
- 38 de Menocal, P.B., 2015. Palaeoclimate: End of the African Humid Period. *Nature Geoscience* 8, 86-87.
- 39 de Menocal, P., Ortiz, J., Guilderson, T., Adkins, J., Sarnthein, M., Baker, L., Yarusinsky, M., 2000. Abrupt onset
40 and termination of the African Humid Period: rapid climate responses to gradual insolation forcing. *Quaternary*
41 *Science Reviews* 19, 347-361.
- 42 Dray, S., Dufour, A.-B., 2007. The ade4 Package: Implementing the Duality Diagram for Ecologists. *Journal of*
43 *Statistical Software* 22, 20.
- 44 Dühnforth, M., Bergner, A.G.N., Trauth, M.H., 2006. Early Holocene water budget of the Nakuru-Elmenteita
45 basin, Central Kenya Rift. *Journal of Paleolimnology* 36, 281-294.

- 1 Dutour, O., 1989. Hommes Fossiles du Sahara. Peuplements holocènes du Mali septentrional. Editions du
2 CNRS, Paris.
- 3 Fleagle, J.G., Assefa, Z., Brown, F.H., Shea, J.J., 2008. Paleoanthropology of the Kibish Formation, southern
4 Ethiopia: Introduction. *Journal of Human Evolution* 55, 360-365.
- 5 Flegontov, P., Changmai, P., Zidkova, A., Logacheva, M.D., Altınışık, N.E., Flegontova, O., Gelfand, M.S.,
6 Gerasimov, E.S., Khrameeva, E.E., Konovalova, O.P., Neretina, T., Nikolsky, Y.V., Starostin, G., Stepanova, V.V.,
7 Travinsky, I.V., Tříška, M., Tříška, P., Tatarinova, T.V., 2016. Genomic study of the Ket: a Paleo-Eskimo-related
8 ethnic group with significant ancient North Eurasian ancestry. *Scientific Reports* 6, 20768.
- 9 Galland, M., 2013. Le premier peuplement des Ameriques: application de la morphométrie géométrique 3D à
10 la variation crânienne actuelle et fossile. Ph.D. Dissertation, Muséum national d'Histoire naturelle.
- 11 Gasse, F., 2000. Hydrological changes in the African tropics since the Last Glacial Maximum. *Quaternary Science*
12 *Reviews* 19, 189-211.
- 13 Gerharz, R., 1994. *Jebel Moya*. Akademie Verlag, Berlin.
- 14 González-José, R., Ramírez-Rozzi, F., Sardi, M., Martínez-Abadías, N., Hernández, M., Pucciarelli, H.M., 2005.
15 Functional-cranial approach to the influence of economic strategy on skull morphology. *American Journal of*
16 *Physical Anthropology* 128, 757-771.
- 17 Gower, J.C., 1975. Generalised Procrustes analysis. *Psychometrika* 40, 33-50.
- 18 Grine, F.E., 2016. The Late Quaternary hominins of Africa: The skeletal evidence from MIS 6-2. In: Jones, S.C.,
19 Stewart, B.A. (Eds.), *Africa from MIS 6-2. Population Dynamics and Paleoenvironments*. Dordrecht, Springer,
20 pp. 323-381.
- 21 Grine, F.E., Bailey, R.M., Harvati, K., Nathan, R.P., Morris, A.G., Henderson, G.M., Ribot, I., Pike, A.W.G., 2007.
22 Late Pleistocene human skull from Hofmeyr, South Africa, and modern human origins. *Science* 315, 226-229.
- 23 Hammer, O., Harper, D.A.T., 2006. *Paleontological Data Analysis*. Blackwell Publishing, Oxford.
- 24 Harvati, K., Weaver, T.D., 2006. Human cranial anatomy and the differential preservation of population history
25 and climate signatures. *Anatomical Record* 288A, 1225-1233.
- 26 Harvati, K., Stringer, C., Grün, R., Aubert, M., Allsworth-Jones, P., Folorunso, C.A., 2011. The Later Stone Age
27 calvaria from Iwo Eleru, Nigeria: Morphology and chronology. *PLoS ONE* 6, e24024.
- 28 Hendrickx, S., 1999. La chronologie de la préhistoire tardive et des débuts de l'histoire de l'Egypte. *Archéo-Nil*
29 9, 13-81.
- 30 Hublin, J.-J., Ben-Ncer, A., Bailey, S.E., Freidline, S.E., Neubauer, S., Skinner, M.M., Bergmann, I., Le Cabec, A.,
31 Benazzi, S., Harvati, K., Gunz, P., 2017. New fossils from Jebel Irhoud, Morocco and the pan-African origin of
32 *Homo sapiens*. *Nature* 546, 289-292.
- 33 Irish, J.D., Konigsberg, L., 2007. The ancient inhabitants of Jebel Moya redux: measures of population affinity
34 based on dental morphology. *International Journal of Osteoarchaeology* 17, 138-156.
- 35 Katz, D.C., Grote, M.N., Weaver, T.D., 2017. Changes in human skull morphology across the agricultural
36 transition are consistent with softer diets in preindustrial farming groups. *Proceedings of the National*
37 *Academy of Sciences USA* 114, 9050-9055.
- 38 Lahr, M., 1996. *The Evolution of Modern Human Diversity: A Study of Cranial Variation*. Cambridge University
39 Press, Cambridge.
- 40 Lahr, M.M., Foley, R.A., 1994. Multiple dispersals and modern human origins. *Evolutionary Anthropology* 3, 48-
41 60.
- 42 Larrasoana, J.C., Roberts, A.P., Rohling, E.J., 2013. Dynamics of green Sahara periods and their role in hominin
43 evolution. *PLoS ONE* 8, e76514.
- 44 Leakey, L.S.B., 1970. *The Stone Age Races of Kenya*. Oxford University Press, London.
- 45 Leakey, R.E.F., 1969. Early *Homo sapiens* remains from the Omo River region of South-west Ethiopia: Faunal
46 remains from the Omo Valley. *Nature* 222, 1132-1133.

- 1 Li, J.Z., Absher, D.M., Tang, H., Southwick, A.M., Casto, A.M., Ramachandran, S., Cann, H.M., Barsh, G.S.,
2 Feldman, M., Cavalli-Sforza, L.L., Myers, R.M., 2008. Worldwide human relationships inferred from genome-
3 wide patterns of variation. *Science* 319, 1100-1104.
- 4 Lieberman, D.E., 2008. Speculations about the selective basis for modern human craniofacial form.
5 *Evolutionary Anthropology* 17, 55-68.
- 6 Liu, H., Prugnolle, F., Manica, A., Balloux, F., 2006. A geographically explicit genetic model of worldwide
7 human-settlement history. *American Journal of Human Genetics* 79, 230-237.
- 8 Malaspina, A.-S., Westaway, M.C., Muller, C., Sousa, V.C., Lao, O., Alves, I., Bergström, A., Athanasiadis, G.,
9 Cheng, J.Y., Crawford, J.E., Heupink, T.H., Macholdt, E., Peischl, S., Rasmussen, S., Schiffels, S., Subramanian, S.,
10 Wright, J.L., Albrechtsen, A., Barbieri, C., Dupanloup, I., Eriksson, A., Margaryan, A., Moltke, I., Pugach, I.,
11 Korneliusson, T.S., Levkivskiy, I.P., Moreno-Mayar, J.V., Ni, S., Racimo, F., Sikora, M., Xue, Y., Aghakhanian, F.A.,
12 Brucato, N., Brunak, S., Campos, P.F., Clark, W., Ellingvåg, S., Fourmile, G., Gerbault, P., Injie, D., Koki, G.,
13 Leavesley, M., Logan, B., Lynch, A., Matisoo-Smith, E.A., McAllister, P.J., Mentzer, A.J., Metspalu, M., Migliano,
14 A.B., Murgha, L., Phipps, M.E., Pomat, W., Reynolds, D., Ricaut, F.-X., Siba, P., Thomas, M.G., Wales, T., Wall,
15 C.M.r., Oppenheimer, S.J., Tyler-Smith, C., Durbin, R., Dortch, J., Manica, A., Schierup, M.H., Foley, R.A., Lahr,
16 M.M., Bowern, C., Wall, J.D., Mailund, T., Stoneking, M., Nielsen, R., Sandhu, M.S., Excoffier, L., Lambert, D.M.,
17 Willerslev, E., 2016. A genomic history of Aboriginal Australia. *Nature* 538, 207-214.
- 18 Mallick, S., Li, H., Lipson, M., Mathieson, I., Gymrek, M., Racimo, F., Zhao, M., Chennagiri, N., Nordenfelt, S.,
19 Tandon, A., Skoglund, P., Lazaridis, I., Sankararaman, S., Fu, Q., Rohland, N., Renaud, G., Erlich, Y., Willems, T.,
20 Gallo, C., Spence, J.P., Song, Y.S., Poletti, G., Balloux, F., van Driem, G., de Knijff, P., Romero, I.G., Jha, A.R.,
21 Behar, D.M., Bravi, C.M., Capelli, C., Hervig, T., Moreno-Estrada, A., Posukh, O.L., Balanovska, E., Balanovsky,
22 O., Karachanak-Yankova, S., Sahakyan, H., Toncheva, D., Yepiskoposyan, L., Tyler-Smith, C., Xue, Y., Abdullah,
23 M.S., Ruiz-Linares, A., Beall, C.M., Di Rienzo, A., Jeong, C., Starikovskaya, E.B., Metspalu, E., Parik, J., Villems, R.,
24 Henn, B.M., Hodoglugil, U., Mahley, R., Sajantila, A., Stamatoyannopoulos, G., Wee, J.T.S., Khusainova, R.,
25 Khusnutdinova, E., Litvinov, S., Ayodo, G., Comas, D., Hammer, M.F., Kivisild, T., Klitz, W., Winkler, C.A.,
26 Labuda, D., Bamshad, M., Jorde, L.B., Tishkoff, S.A., Watkins, W.S., Metspalu, M., Dryomov, S., Sukernik, R.,
27 Singh, L., Thangaraj, K., Pääbo, S., Kelso, J., Patterson, N., Reich, D., 2016. The Simons Genome Diversity
28 Project: 300 genomes from 142 diverse populations. *Nature* 538, 201-206.
- 29 Marom, A., McCullagh, J.S., Higham, T.F., Sinitsyn, A.A., Hedges, R.E., 2012. Single amino acid radiocarbon
30 dating of Upper Paleolithic modern humans. *Proceedings of the National Academy of Sciences USA* 109, 6878-
31 6881.
- 32 Mirazón Lahr, M., 2016. The shaping of human diversity: filters, boundaries and transitions. *Philosophical*
33 *Transactions of the Royal Society B: Biological Sciences* 371, 1698.
- 34 Mirazón Lahr, M., Foley, R.A., 2016. Human evolution in Late Quaternary Eastern Africa. In: Jones, S.C.,
35 Stewart, B.A. (Eds.), *Africa From MIS 6-2. Population Dynamics and Paleoenvironments*. Dordrecht, Springer,
36 pp. 215-231.
- 37 Mirazón Lahr, M., Rivera, F., Power, R.K., Mounier, A., Copsey, B., Crivellaro, F., Edung, J.E., Fernandez, J.M.M.,
38 Kiarie, C., Lawrence, J., Leakey, A., Mbua, E., Miller, H., Muigai, A., Mukhongo, D.M., Van Baelen, A., Wood, R.,
39 Schwenninger, J.L., Grün, R., Achyuthan, H., Wilshaw, A., Foley, R.A., 2016. Inter-group violence among early
40 Holocene hunter-gatherers of West Turkana, Kenya. *Nature* 529, 394-398.
- 41 Mondal, M., Casals, F., Xu, T., Dall'Olio, G.M., Pybus, M., Netea, M.G., Comas, D., Laayouni, H., Li, Q.,
42 Majumder, P.P., Bertranpetit, J., 2016. Genomic analysis of Andamanese provides insights into ancient human
43 migration into Asia and adaptation. *Nature Genetics* 48, 1066-1070.
- 44 Mounier, A., Marchal, F., Condemi, S., 2009. Is *Homo heidelbergensis* a distinct species? New insight on the
45 Mauer mandible. *Journal of Human Evolution* 56, 219-246.
- 46 Nicholson, E., Harvati, K., 2006. Quantitative analysis of human mandibular shape using three-dimensional
47 geometric morphometrics. *American Journal of Physical Anthropology* 131, 368-383.
- 48 Noback, M.L., Harvati, K., 2015a. The contribution of subsistence to global human cranial variation. *Journal of*
49 *Human Evolution* 80, 34-50.

- 1 Noback, M.L., Harvati, K., 2015b. Covariation in the human masticatory apparatus. *Anatomical Record* 298, 64-
2 84.
- 3 Noback, M.L., Harvati, K., Spoor, F., 2011. Climate-related variation of the human nasal cavity. *American*
4 *Journal of Physical Anthropology* 145, 599-614.
- 5 Oakley, K.P., 1961. Bone harpoon from Gamble's Cave, Kenya. *The Antiquaries Journal* 41, 86-87.
- 6 Pagani, L., Lawson, D.J., Jagoda, E., Mörseburg, A., Eriksson, A., Mitt, M., Clemente, F., Hudjashov, G.,
7 DeGiorgio, M., Saag, L., Wall, J.D., Cardona, A., Mägi, R., Sayres, M.A.W., Kaewert, S., Inchley, C., Scheib, C.L.,
8 Järve, M., Karmin, M., Jacobs, G.S., Antao, T., Iliescu, F.M., Kushniarevich, A., Ayub, Q., Tyler-Smith, C., Xue, Y.,
9 Yunusbayev, B., Tambets, K., Mallick, C.B., Saag, L., Pocheshkhova, E., Andriadze, G., Muller, C., Westaway,
10 M.C., Lambert, D.M., Zoraqi, G., Turdikulova, S., Dalimova, D., Sabitov, Z., Sultana, G.N.N., Lachance, J.,
11 Tishkoff, S., Momynaliev, K., Isakova, J., Damba, L.D., Gubina, M., Nymadawa, P., Evseeva, I., Atramentova, L.,
12 Utevska, O., Ricaut, F.-X., Brucato, N., Sudoyo, H., Letellier, T., Cox, M.P., Barashkov, N.A., Škaro, V.,
13 Mulahasanović, L., Primorac, D., Sahakyan, H., Mormina, M., Eichstaedt, C.A., Lichman, D.V., Abdullah, S.,
14 Chaubey, G., Wee, J.T.S., Mihailov, E., Karunas, A., Litvinov, S., Khusainova, R., Ekomasova, N., Akhmetova, V.,
15 Khidiyatova, I., Marjanović, D., Yepiskoposyan, L., Behar, D.M., Balanovska, E., Metspalu, A., Derenko, M.,
16 Malyarchuk, B., Voevoda, M., Fedorova, S.A., Osipova, L.P., Lahr, M.M., Gerbault, P., Leavesley, M., Migliano,
17 A.B., Petraglia, M., Balanovsky, O., Khusnutdinova, E.K., Metspalu, E., Thomas, M.G., Manica, A., Nielsen, R.,
18 Villems, R., Willerslev, E., Kivisild, T., Metspalu, M., 2016. Genomic analyses inform on migration events during
19 the peopling of Eurasia. *Nature* 538, 238-241.
- 20 Protsch, R., 1978. The chronological position of Gamble's Cave II and Bromhead's Site (Elmenteita) of the Rift
21 Valley, Kenya. *Journal of Human Evolution* 7, 101-109.
- 22 Raghavan, M., DeGiorgio, M., Albrechtsen, A., Moltke, I., Skoglund, P., Korneliussen, T.S., Grønnøw, B., Appelt,
23 M., Gulløv, H.C., Friesen, T.M., Fitzhugh, W., Malmström, H., Rasmussen, S., Olsen, J., Melchior, L., Fuller, B.T.,
24 Fahrni, S.M., Stafford, T., Grimes, V., Renouf, M.A.P., Cybulski, J., Lynnerup, N., Lahr, M.M., Britton, K., Knecht,
25 R., Arneborg, J., Metspalu, M., Cornejo, O.E., Malaspinas, A.-S., Wang, Y., Rasmussen, M., Raghavan, V.,
26 Hansen, T.V.O., Khusnutdinova, E., Pierre, T., Dneprovsky, K., Andreasen, C., Lange, H., Hayes, M.G., Coltrain, J.,
27 Spitsyn, V.A., Götherström, A., Orlando, L., Kivisild, T., Villems, R., Crawford, M.H., Nielsen, F.C., Dissing, J.,
28 Heinemeier, J., Meldgaard, M., Bustamante, C., O'Rourke, D.H., Jakobsson, M., Gilbert, M.T.P., Nielsen, R.,
29 Willerslev, E., 2014. The genetic prehistory of the New World Arctic. *Science* 345, 1255832.
- 30 Rak, Y., Ginzburg, A., Geffen, E., 2002. Does *Homo neanderthalensis* play a role in modern human ancestry?
31 The mandibular evidence. *American Journal of Physical Anthropology* 119, 199–204.
- 32 Reyes-Centeno, H., Ghirotto, S., Détroit, F., Grimaud-Hervé, D., Barbujani, G., Harvati, K., 2014. Genomic and
33 cranial phenotype data support multiple modern human dispersals from Africa and a southern route into Asia.
34 *Proceedings of the National Academy of Sciences USA* 111, 7248-7253.
- 35 Robbins, L.H., 1974. The Lothagam site: a Late Stone Age fishing settlement in the Lake Rudolf basin, Kenya.
36 East Lansing, Michigan State University Museum.
- 37 Robbins, L.H., 1975. Bone artefacts from the Lake Rudolf Basin, East Africa. *Current Anthropology* 16, 632-633.
- 38 Robbins, L.H., 2006. Lake Turkana archaeology: The Holocene. *Ethnohistory* 53, 71-93.
- 39 Rohlf, F.J., Slice, D.E., 1990. Extensions of the Procrustes method for the optimal superimposition of
40 landmarks. *Systematic Zoology* 39, 40-59.
- 41 Rosas, A., 1992. Ontogenia y Filogenia de la Mandíbula en la Evolución de los Homínidos. Aplicación de un
42 Modelo de Morfogénesis a las Mandíbulas Fósiles de Atapuerca. Ph.D. Dissertation, Complutense University.
- 43 Roseman, C.C., Weaver, T.D., 2004. Multivariate apportionment of global human craniometric diversity.
44 *American Journal of Physical Anthropology* 125, 257-263.
- 45 Saitou, N., Nei, M., 1987. The neighbor-joining method: a new method for reconstructing phylogenetic trees.
46 *Molecular Biology and Evolution* 4, 406-425.
- 47 Schlebusch, C.M., Malmström, H., Günther, T., Sjödin, P., Coutinho, A., Edlund, H., Munters, A.R., Steyn, M.,
48 Soodyall, H., Lombard, M., Jakobsson, M., 2017. Southern African ancient genomes estimate modern human
49 divergence to 350,000 to 260,000 years ago. *Science* 358, 652-655.

- 1 Schliep, K.P., 2011. phangorn: phylogenetic analysis in R. *Bioinformatics* 27, 592-593.
- 2 Schwartz, G.T., Tattersall, I., 2000. The human chin revisited: what is it and who has it? *Journal of Human*
3 *Evolution* 38, 367-409.
- 4 Simon, C., 1989. Les populations Kerma - Evolution interne et relations historiques dans le contexte Egypto-
5 Nubiens. *Archéologie du Nil Moyen* 3, 139-147.
- 6 Smith, F.H., 1982. Upper Pleistocene hominid evolution in South-Central Europe: A review of the evidence and
7 analysis of trends. *Current Anthropology* 23, 666-703.
- 8 Smith, H.F., 2009. Which cranial regions reflect molecular distances reliably in humans? Evidence from three-
9 dimensional morphology. *American Journal of Human Biology* 21, 36-47.
- 10 Sonnevile-Bordes, D., 1959. Position stratigraphique et chronologique relative des restes humains du
11 Paléolithique Supérieur entre Loire et Pyrénées. *Annales de Paléontologie (Vertébrés)* 45, 19-51.
- 12 Stock, J.T., Migliano, A.B., 2009. Stature, mortality, and life history among indigenous populations of the
13 Andaman Islands, 1871-1986. *Current Anthropology* 50, 713-725.
- 14 Street, M., Terberger, T., Orschiedt, J., 2006. A critical review of the German Paleolithic hominin record.
15 *Journal of Human Evolution* 51, 551-579.
- 16 Svoboda, A.J., 2008. The Upper Paleolithic burial area at Předmostí: ritual and taphonomy. *Journal of Human*
17 *Evolution* 54, 15-33.
- 18 Tishkoff, S.A., Reed, F.A., Friedlaender, F.R., Ehret, C., Ranciaro, A., Froment, A., Hirbo, J.B., Awomoyi, A.A.,
19 Bodo, J.-M., Doumbo, O., Ibrahim, M., Juma, A.T., Kotze, M.J., Lema, G., Moore, J.H., Mortensen, H., Nyambo,
20 T.B., Omar, S.A., Powell, K., Pretorius, G.S., Smith, M.W., Thera, M.A., Wambebe, C., Weber, J.L., Williams,
21 S.M., 2009. The genetic structure and history of Africans and African Americans. *Science* 324, 1035-1044.
- 22 Trinkaus, E., Svoboda, J., 2006. *Early Modern Human Evolution in Central Europe*. Oxford University Press, New
23 York.
- 24 Tryon, C.A., Crevecoeur, I., Faith, J.T., Ekshtain, R., Nivens, J., Patterson, D., Mbua, E.N., Spoor, F., 2015. Late
25 Pleistocene age and archaeological context for the hominin calvaria from GvJm-22 (Lukenya Hill, Kenya).
26 *Proceedings of the National Academy of Sciences USA* 112, 2682-2687.
- 27 von Cramon-Taubadel, N., 2009a. Congruence of individual cranial bone morphology and neutral molecular
28 affinity patterns in modern humans. *American Journal of Physical Anthropology* 140, 205-215.
- 29 von Cramon-Taubadel, N., 2009b. Revisiting the homology hypothesis: the impact of phenotypic plasticity on
30 the reconstruction of human population history from craniometric data. *Journal of Human Evolution* 57, 179-
31 190.
- 32 von Cramon-Taubadel, N., 2011. Global human mandibular variation reflects differences in agricultural and
33 hunter-gatherer subsistence strategies. *Proceedings of the National Academy of Sciences USA* 108, 19546-
34 19551.
- 35 von Cramon-Taubadel, N., 2014. Evolutionary insights into global patterns of human cranial diversity:
36 population history, climatic and dietary effects. *Journal of Anthropological Sciences* 92, 43-77.
- 37 Weninger, B., Joris, O., 2004. Glacial radiocarbon calibration. The CalPal Program. In: Higham, T., Ramsey, C.B.,
38 Owen, C. (Eds.), *Radiocarbon and Archaeology*. Proceedings of the 4th Symposium. Oxford University School
39 *Archaeology Monograph* 62, Oxford, pp. 9-15.
- 40 White, T.D., Asfaw, B., DeGusta, D., Gilbert, W.H., Richards, G.D., Suwa, G., Howell, F.C., 2003. Pleistocene
41 *Homo sapiens* from Middle Awash, Ethiopia. *Nature* 423, 742-747.
- 42 White, T.D., Black, T.M., Folkens, P.A., 2011. *Human Osteology Third Edition*. Academic Press, Oxford.
- 43 Zaidi, A.A., Mattern, B.C., Claes, P., McEcoy, B., Hughes, C., Shriver, M.D., 2017. Investigating the case of
44 human nose shape and climate adaptation. *PLoS Genet.* 13, e1006616.

45

46

1 **Figures legends**

2

3 **Figure 1**

4 Four of the mandibles from the site of Nataruk (West Turkana, Kenya) showed in norma lateralis,
5 norma facialis, norma occipitalis and normal superalis (from left to right). (A) KNM-WT 71251, (B)
6 KNM-WT 71253, (C) KNM-WT 71254, (D) KNM-WT 71255. The mandibles are scaled in relation to
7 each other.

8

9 **Figure 2**

10 Four of the mandibles from the site of Nataruk (West Turkana, Kenya) showed in norma lateralis,
11 norma facialis, norma occipitalis and normal superalis (from left to right). (A) KNM-WT 71256, (B)
12 KNM-WT 71257, (C) KNM-WT 71263, (D) KNM-WT 71264. The mandibles are scaled in relation to
13 each other. Norma lateralis is reversed for KNM-WT 71256.

14

15 **Figure 3**

16 Boxplots showing centroid size according to the three different grouping of our sample. (A)
17 worldwide populations, (B) worldwide meta-populations, and (C) African populations. The size of the
18 Nataruk mandible is similar to Pleistocene specimens, and to the Lothagam sample.

19

20

21 **Figure 4**

22 bgPCA showing the variation in shape within the mandibular sample grouped per worldwide
23 populations. The ellipses represent the 90% confidence interval for the estimated distribution of the
24 specimens of each population. Each specimen is linked to the centroid of its group of origin. The
25 Nataruk specimens are closer in shape to the Lothagam (red) and late Pleistocene Afalou and
26 Tavoralt (brown) specimens. NK2 stands for Nazlet Khater 2.

27

28 **Figure 5**

29 bgPCA showing the variation in shape within the mandibular sample grouped per worldwide meta-
30 populations. The ellipses represent the 90% confidence interval for the estimated distribution of the
31 specimens of each population. Each specimen is linked to the centroid of its group of origin. The
32 Nataruk specimens are closer in shape to the Kenyan Holocene (red) and North Africa Pleistocene
33 (brown) specimens.

34

1 **Figure 6**

2 bgPCA showing the variation in shape within the mandibular sample grouped per African
3 populations. The ellipses represent the 90% confidence interval for the estimated distribution of the
4 specimens of each population. Each specimen is linked to the centroid of its group of origin. The
5 Nataruk specimens are closer in shape to the Lothagam (red) and Nazlet Khater 2 (i.e., NK2, brown)
6 specimens.

7

8 **Figure 7**

9 PCAs run on the mean shape of each population and associated unrooted Neighbour-Joining trees
10 with a 10,000 replications bootstrap. (A) worldwide populations, (B) worldwide meta-populations,
11 and (C) African populations. In each tree, the Nataruk and Lothagam specimens (Holocene Kenya in
12 7B) cluster together.

13

1 **Table legends**

2

3 **Table 1: Specimens used in the study**

4 Bold type indicates that the original fossils were examined.

5 *The sex ratio corresponds to the number of females divided by the total population number.

6 ^a Individual fossil specimens that compose this sample are listed in Table 2.

7 ^b References for chronology are listed in Table 2.

8

9 **Table 2. Description of fossil specimens.**

10 Bold type indicates that the original fossils were examined.

11

12 **Table 3. Comparison of the centroid size for each meta-population and population of the study.**

13

14 **Table 4. Between groups PCA – worldwide sample. *p*-values of pairwise group differences – based**
15 **on permutation testing.**

16 Bold types: *p*-values > 0.05, indicating that the pairwise group difference is not significant.

17

18 **Table 5. Between groups PCA – worldwide meta-populations. *p*-values of pairwise group**
19 **differences – based on permutation testing.**

20 Bold types: *p*-values > 0.05, indicating that the pairwise group difference is not significant.

21

22 **Table 6. Between groups PCA – African sample. *p*-values of pairwise group differences – based on**
23 **permutation testing.**

24 Bold types: *p*-values > 0.05, indicating that the pairwise group difference is not significant.

25

1 **Supplementary Online Material :**

2

3 **SOM-1**

4

5 **Sample description**

6

7 **Table S1. Description of the specimens studied in the study**

8 ^a '?' indicates when the sex has been established using secondary sexual characters of the skull (see,
9 Buikstra and Ubelaker, 1994; White et al., 2011).

10 ^b Indicates where the specimens are kept and in the case of Nazlet Khater whom gave access to the
11 CT scan: DC = Duckworth Collection, Cambridge, UK; IPH = Institut de Paléontologie Humaine, Paris,
12 France; MH = Musée de l'Homme, Paris, France; Brno = Anthropos Institute, Brno, Czech Republic;
13 ORS = Open Scan Research Archive, University of Pennsylvania Museum of Archeology and
14 Anthropology, USA; NMK = National Museums of Kenya, Nairobi; IC = Isabelle Crevecoeur.

15 ^c Percentage of missing landmarks that were estimated using TPS.

16

17 **Table S2. Description of the landmarks used in the study (see Fig. 4)**

18

19 **Between group PCA and PCA**

20

21 **Table S3. Between groups PCs eigenvalues and variance** Description of the bgPCs of the bgPCAs run
22 on Procrustes residuals according to worldwide populations, worldwide meta-populations and
23 African-populations.

24

25 **Table C.2. PCAs – eigenvalues and variance**

26 Description of the PCs of the PCAs run on the mean shape of the populations according to worldwide
27 populations, worldwide meta-populations and African-populations.

28

29 **SOM-2**

30 **Test of TPS performance in estimating the missing landmarks**

31 PCs scores of the subsamples used to test the performance of TPS in estimating landmarks, along
32 with T-test results on mean and variance for each estimated landmark. The differences in mean and
33 variance are not significant.

34

1 **Figure Legend**

2 **Figure S1.**

3 PCA of 30 subsamples of 30 specimens without missing landmarks. Each of the missing landmarks
4 estimated through TPS in the main analysis has been deleted in one of the subsamples, before being
5 estimated through TPS, creating 31 groups of 30 specimens. Each of the group was given a colour
6 code on the PCA graphs. The 930 resultant specimens were aligned (i.e., GPA) and a PCA was run: (A)
7 PCA PC1 and 2; (B) PC3 and 4; (C) PC5 and 6; (D) missing landmarks estimated. Estimation of missing
8 landmarks through TPS does not affect fundamentally the results of the PCA.

Table 1: Specimens used in the study

Meta-populations and Populations	<i>n</i>	Sex ratio*	Provenance	Chronology	Reference (chronology)
Nataruk	8	0.36	Kenya	10,500-9,500 BP	(Mirazón Lahr et al., 2016)
<i>Extant Sub-Sahara (n=63)</i>					
Haya	24	0.33	Tanzania	19th century	-
Somali Daarod (14); Ainhao (2); Hahr Jalo (2)	18	0.11	Somalia	20th century	-
Khoisan	11	0.54	South Africa	19th century	-
Bantu	10	0	South Africa	19th century	-
<i>Extant Asia (n=43)</i>					
Andamanese	11	0.54	Andaman Islands, India	19th century	-
Nicobarese	11	0.45	Nicobar Islands, India	19th century	-
Chinese	12	0.1	China	19th century	-
Sri Lankan Veddah (4); Singhalese (3); Tamil (2)	9	0.22	Sri Lanka	19th century	-
<i>Extant Oceania (n=37)</i>					
Papuan	16	0.38	Papua New Guinea	19th century	-
Australian	21	0.43	Australia	19th century	-
<i>Extant European (n=17)</i>					
European	17	0.47	Europe	19th century	-
<i>Extant Inuit (n=18)</i>					
Inuit	18	0.4	Greenland	19th century	-
<i>Nile Valley (n=63)</i>					
Kerma (Nubian)	16	0.5	Sudan	3,750-3,480 BP	(Collett, 1933; Simon, 1989)
Jebel Moya (Nubian)	14	0.57	Sudan	5,000-2,100 BP	(Brass and Schwenniger, 2013)
Badari (Pre-Dynastic)	18	0.39	Egypt	5,440-5,110 BP	(Hendrickx, 1999)
Naqada (Pre-Dynastic)	15	0.47	Egypt	5,000-4,000 BP	(Hendrickx, 1999)
<i>Holocene Kenya (n=14)</i>					
Lothagam	7	0.43	Kenya	9,000-6,000 BP	(Robbins, 1974)
Central Rift^a	7	0.29	Kenya	8,210-5,000 BP	- ^b
<i>Pleistocene North Africa (n=38)</i>					
Taforalt - Grotte des Pigeons	20	0.35	Morocco	15,000-10,000 BP	(Aoudia-Chouakri, 2013)
Afalou Bou Rummel	17	0.12	Algeria	15,000-11,000 BP	(Aoudia-Chouakri, 2013)
Nazlet Khater 2	1	0	Egypt	35,000 BP	(Crevecoeur, 2006)
<i>Pleistocene Europe (n=11)</i>					
Europe^a	11	0.5	-	50,000-12,000 BP	- ^b
Total	312	0.35			

*The sex ratio corresponds to the number of females divided by the total population number.

^a Individual fossil specimens that compose this sample are listed in Table 2.

^b References for chronology are listed in Table 2.

Table 2: Description of fossil specimens

Specimen	Sex	Site	Chronology	Chronology references
<i>Holocene</i>		<i>Nataruk</i>		
KNM-WT 71251	M	Nataruk, West Turkana, Kenya	10,500-9,500 BP	(Mirazón Lahr et al., 2016)
KNM-WT 71253	M	Nataruk, West Turkana, Kenya	10,500-9,500 BP	(Mirazón Lahr et al., 2016)
KNM-WT 71254	F?	Nataruk, West Turkana, Kenya	10,500-9,500 BP	(Mirazón Lahr et al., 2016)
KNM-WT 71255	F	Nataruk, West Turkana, Kenya	10,500-9,500 BP	(Mirazón Lahr et al., 2016)
KNM-WT 71256	F	Nataruk, West Turkana, Kenya	10,500-9,500 BP	(Mirazón Lahr et al., 2016)
KNM-WT 71257	M	Nataruk, West Turkana, Kenya	10,500-9,500 BP	(Mirazón Lahr et al., 2016)
KNM-WT 71263	M	Nataruk, West Turkana, Kenya	10,500-9,500 BP	(Mirazón Lahr et al., 2016)
KNM-WT 71264	M	Nataruk, West Turkana, Kenya	10,500-9,500 BP	(Mirazón Lahr et al., 2016)
		<i>Lothagam</i>		
KNM-LT 13702E	M?	Lothagam, West Turkana, Kenya	9,000-6,000 BP	(Robbins, 1974)
KNM-LT 13704B	M?	Lothagam, West Turkana, Kenya	9,000-6,000 BP	(Robbins, 1974)
KNM-LT 27710	M?	Lothagam, West Turkana, Kenya	9,000-6,000 BP	(Robbins, 1974)
KNM-LT 27712C	M?	Lothagam, West Turkana, Kenya	9,000-6,000 BP	(Robbins, 1974)
KNM-LT 27714	F?	Lothagam, West Turkana, Kenya	9,000-6,000 BP	(Robbins, 1974)
KNM-LT 27715B	F?	Lothagam, West Turkana, Kenya	9,000-6,000 BP	(Robbins, 1974)
KNM-LT 27717B	F?	Lothagam, West Turkana, Kenya	9,000-6,000 BP	(Robbins, 1974)
		<i>Central Rift Valley</i>		
Elmenteita A	M	Elmenteita, Bromhead, Kenya	7,410±160 BP	(Protsch, 1978)
Elmenteita D	M	Elmenteita, Bromhead, Kenya	7,410±160 BP	(Protsch, 1978)
Elmenteita F1	F	Elmenteita, Bromhead, Kenya	7,410±160 BP	(Protsch, 1978)
Gamble's Cave 4	M	Gamble's Cave, Kenya	8,210±260 BP	(Protsch, 1978)
Gamble's Cave 5	M	Gamble's Cave, Kenya	8,210±260 BP	(Protsch, 1978)
Nakuru IX	F	Nakuru, Kenya	Early Pastoral Neolithic	(Leakey, 1970)
Willey Kopje II	M	Willey Kopje, Kenya	Early Pastoral Neolithic	(Leakey, 1970)
<i>Pleistocene</i>		<i>Afalou</i>		
Afalou A.1	M	Afalou Bou Rhummel, Algeria	15,000-11,000 BP	(Aoudia-Chouakri, 2013)
Afalou A.2	M	Afalou Bou Rhummel, Algeria	15,000-11,000 BP	(Aoudia-Chouakri, 2013)
Afalou A.3	F	Afalou Bou Rhummel, Algeria	15,000-11,000 BP	(Aoudia-Chouakri, 2013)
Afalou A.5	F?	Afalou Bou Rhummel, Algeria	15,000-11,000 BP	(Aoudia-Chouakri, 2013)
Afalou A.10	M	Afalou Bou Rhummel, Algeria	15,000-11,000 BP	(Aoudia-Chouakri, 2013)
Afalou A.12	M?	Afalou Bou Rhummel, Algeria	15,000-11,000 BP	(Aoudia-Chouakri, 2013)
Afalou A.13	M	Afalou Bou Rhummel, Algeria	15,000-11,000 BP	(Aoudia-Chouakri, 2013)
Afalou A.14	M	Afalou Bou Rhummel, Algeria	15,000-11,000 BP	(Aoudia-Chouakri, 2013)
Afalou A.28	M	Afalou Bou Rhummel, Algeria	15,000-11,000 BP	(Aoudia-Chouakri, 2013)
Afalou A.30	M?	Afalou Bou Rhummel, Algeria	15,000-11,000 BP	(Aoudia-Chouakri, 2013)
Afalou A.34	M?	Afalou Bou Rhummel, Algeria	15,000-11,000 BP	(Aoudia-Chouakri, 2013)
Afalou A.46	M?	Afalou Bou Rhummel, Algeria	15,000-11,000 BP	(Aoudia-Chouakri, 2013)
Afalou A.47	M?	Afalou Bou Rhummel, Algeria	15,000-11,000 BP	(Aoudia-Chouakri, 2013)
Afalou A.48	M?	Afalou Bou Rhummel, Algeria	15,000-11,000 BP	(Aoudia-Chouakri, 2013)
Afalou A.49	M?	Afalou Bou Rhummel, Algeria	15,000-11,000 BP	(Aoudia-Chouakri, 2013)
Afalou B 4	M?	Afalou Bou Rhummel, Algeria	15,000-11,000 BP	(Aoudia-Chouakri, 2013)
Afalou Md 2-3	M?	Afalou Bou Rhummel, Algeria	15,000-11,000 BP	(Aoudia-Chouakri, 2013)

<i>Taforalt</i>				
Taf I	F?	Taforalt, <i>Grotte des Pigeons</i> , Morocco	15,000-10,000 BP	(Aoudia-Chouakri, 2013)
Taf IX	M	Taforalt, <i>Grotte des Pigeons</i> , Morocco	15,000-10,000 BP	(Aoudia-Chouakri, 2013)
Taf VIII PB	M	Taforalt, <i>Grotte des Pigeons</i> , Morocco	15,000-10,000 BP	(Aoudia-Chouakri, 2013)
Taf XI-B.C2	M	Taforalt, <i>Grotte des Pigeons</i> , Morocco	15,000-10,000 BP	(Aoudia-Chouakri, 2013)
Taf XI-C1	M?	Taforalt, <i>Grotte des Pigeons</i> , Morocco	15,000-10,000 BP	(Aoudia-Chouakri, 2013)
Taf XII-C1	M	Taforalt, <i>Grotte des Pigeons</i> , Morocco	15,000-10,000 BP	(Aoudia-Chouakri, 2013)
Taf XIV	F?	Taforalt, <i>Grotte des Pigeons</i> , Morocco	15,000-10,000 BP	(Aoudia-Chouakri, 2013)
Taf XIX-C1	F?	Taforalt, <i>Grotte des Pigeons</i> , Morocco	15,000-10,000 BP	(Aoudia-Chouakri, 2013)
Taf XV-C2	M?	Taforalt, <i>Grotte des Pigeons</i> , Morocco	15,000-10,000 BP	(Aoudia-Chouakri, 2013)
Taf XV-C5	M	Taforalt, <i>Grotte des Pigeons</i> , Morocco	15,000-10,000 BP	(Aoudia-Chouakri, 2013)
Taf XVI-C2	F?	Taforalt, <i>Grotte des Pigeons</i> , Morocco	15,000-10,000 BP	(Aoudia-Chouakri, 2013)
Taf XVII-C2	F	Taforalt, <i>Grotte des Pigeons</i> , Morocco	15,000-10,000 BP	(Aoudia-Chouakri, 2013)
Taf XVIII	M?	Taforalt, <i>Grotte des Pigeons</i> , Morocco	15,000-10,000 BP	(Aoudia-Chouakri, 2013)
Taf XX-C1	M?	Taforalt, <i>Grotte des Pigeons</i> , Morocco	15,000-10,000 BP	(Aoudia-Chouakri, 2013)
Taf XX-C2	F?	Taforalt, <i>Grotte des Pigeons</i> , Morocco	15,000-10,000 BP	(Aoudia-Chouakri, 2013)
Taf XXI	M?	Taforalt, <i>Grotte des Pigeons</i> , Morocco	15,000-10,000 BP	(Aoudia-Chouakri, 2013)
Taf XXV-C3	F?	Taforalt, <i>Grotte des Pigeons</i> , Morocco	15,000-10,000 BP	(Aoudia-Chouakri, 2013)
Taf XXV.2	M?	Taforalt, <i>Grotte des Pigeons</i> , Morocco	15,000-10,000 BP	(Aoudia-Chouakri, 2013)
Taf XXVII-C1	M?	Taforalt, <i>Grotte des Pigeons</i> , Morocco	15,000-10,000 BP	(Aoudia-Chouakri, 2013)
Taf XXVII-C2	M	Taforalt, <i>Grotte des Pigeons</i> , Morocco	15,000-10,000 BP	(Aoudia-Chouakri, 2013)
<i>Europe</i>				
Brno 3	F	Brno, Czech Republic	26,300 BP	(Smith, 1982)
Dolní Věstonice 3	F	Dolní Věstonice, Czech Republic	29,000-26,000 BP	(Trinkaus and Svoboda, 2006)
Dolní Věstonice 13	M	Dolní Věstonice, Czech Republic	29,000-26,000 BP	(Trinkaus and Svoboda, 2006)
Dolní Věstonice 15	M	Dolní Věstonice, Czech Republic	29,000-26,000 BP	(Trinkaus and Svoboda, 2006)
Pavlov I	M	Pavlov, Czech Republic	29,000-26,000 BP	(Weninger and Joris, 2004)
Předmostí 4	F	Předmostí, Czech Republic	26,000 BP	(Svoboda, 2008)
Předmostí 3	M	Předmostí, Czech Republic	26,000 BP	(Svoboda, 2008)
Abri Pataud 1	F	Abri Pataud, France	21,000 BP	(Bricker and Mellars, 1987)
Chancelade	M	Chancelade, France	17,000-12,000 BP	(Sonneville-Bordes, 1959)
Kostenski 14	M	Kostenski-Borshchevo, Russia	38,700-36,200 BP	(Marom et al., 2012)
Oberkassel 2	F	Oberkassel, Germany	~12,000 BP	(Street et al., 2006)
<i>Nazlet Khater</i>				
Nazlet Khater 2	M	Nazlet Khater, Egypt	35,000 BP	(Crevecoeur, 2006)

Bold type indicates that the original fossils were examined.

Table 3

Comparison of the centroid size for each meta-population and population of the study.

Meta-populations	Populations	Africans	Centroid Size			
			Mean	Max	Min	sd
Nataruk (n = 8)			250.85	258.81	228.37	13.05
Nile Valley (n = 63)			227.69	261.56	201.68	13.21
	Kenya (n = 16)		237.11	257.05	222.76	8.18
	Jebel Moya (n = 14)		230.46	261.56	202.98	16.28
	Naqada (n = 15)		226.32	250.17	202.32	10.74
	Badari (n = 18)		218.31	243.76	201.68	9.76
Sub-Saharan (n = 68)			233.06	260.76	196.63	13.32
	Haya (n = 24)		237.84	259.72	213.32	10.36
	Somali (n = 18)		232.74	244.98	206.62	9.48
	Khoisan (n = 11)		216.96	242.83	196.63	14.75
	Bantu (n = 10)		239.89	260.76	221.57	10.33
Asia (n = 43)			223.54	241.15	191.34	12.39
	China (n = 12)		234.20	241.16	221.46	5.76
	Sri Lanka (n = 9)		225.83	240.22	209.09	9.82
	Andaman (n = 11)		209.90	223.92	191.34	10.38
	Nicobar (n = 11)		223.67	236.01	203.35	8.84
Oceania (n = 37)			231.61	251.72	209.39	10.51
	Papua (n = 16)		230.21	251.72	216.01	11.89
	Australia (n = 21)		232.68	250.14	209.39	9.50
Europe (n = 17)			231.89	246.51	218.38	8.03
Inuit (n = 18)			233.59	249.51	209.72	9.01
Holocene Kenya (n = 14)			246.63	277.94	226.16	15.86
	Holocene Central Rift (n = 7)		238.66	261.07	226.17	11.85
	Elmenteita (n = 3)		240.80	261.07	226.16	18.12
	Gamble's Cave (n = 2)		231.02	233.69	228.35	3.78
	Nakuru IX		243.99	--	--	--
	Willey Kopje II		242.18	--	--	--
	Lothagam (n = 7)		254.60	277.95	231.26	16.01
Pleistocene Europe (n = 11)			233.194	252.96	215.51	13.57
Pleistocene North Africa (n = 38)			245.08	272.89	215.90	14.14
	Afalou (n = 17)		242.87	264.13	218.31	11.20
	Taforalt (n = 20)		246.37	272.89	215.90	16.43
	Nazlet Khater 2		256.92	--	--	--

Table 4. Between groups PCA – worldwide sample. p -values of pairwise group differences – based on permutation testing

	Kerma	Jebel Moya	Naqada	Badari	Haya	Somali	Khoisan	Bantu	China	Sri Lanka	Andaman	Nicobar	Papua	Australia	Europe	Inuit	Holocene Central Rift	Lothagam	Pleistocene Europe	Afalou	Taforalt	Nazlet Khater 2
Jebel Moya	0.0004																					
Naqada	0.2664	0.0065																				
Badari	0.0004	0.1373	0.1886																			
Haya	0.0001	0.0125	0.0002	0.0718																		
Somali	0.0002	0.0376	0.0192	0.1417	0.0016																	
Khoisan	0.0001	0.0913	0.0001	0.0172	0.0340	0.0017																
Bantu	0.0012	0.2409	0.0315	0.2023	0.7179	0.0856	0.1197															
China	0.0004	0.0516	0.0058	0.0040	0.0012	0.0003	0.0050	0.0365														
Sri Lanka	0.0004	0.0007	0.0056	0.0009	0.0001	0.0001	0.0002	0.0044	0.0886													
Andaman	0.0001	0.0166	0.0003	0.0049	0.0286	0.0003	0.0214	0.1457	0.1585	0.2219												
Nicobar	0.0001	0.0135	0.0002	0.0029	0.0184	0.0001	0.0140	0.1097	0.2199	0.0326	0.7160											
Papua	0.0001	0.0014	0.0033	0.0001	0.0001	0.0001	0.0001	0.0040	0.0554	0.0365	0.0320	0.0017										
Australia	0.0223	0.0001	0.1790	0.0003	0.0001	0.0002	0.0001	0.0010	0.0002	0.0001	0.0001	0.0001	0.0034									
Europe	0.0001	0.0218	0.0001	0.0225	0.0007	0.0087	0.0761	0.0245	0.0005	0.0001	0.0001	0.0001	0.0001	0.0001								
Inuit	0.0286	0.0321	0.2117	0.0247	0.0001	0.0042	0.0001	0.0486	0.0278	0.0062	0.0046	0.0055	0.0850	0.4329	0.0001							
Holocene Central Rift	0.0131	0.0112	0.1004	0.0805	0.0087	0.1086	0.0066	0.2595	0.0012	0.0001	0.0012	0.0006	0.0008	0.0267	0.0104	0.0339						
Lothagam	0.0001	0.0001	0.0001	0.0001	0.0001	0.0001	0.0001	0.0002	0.0001	0.0001	0.0001	0.0001	0.0001	0.0001	0.0001	0.0001	0.0004					
Pleistocene Europe	0.0001	0.0053	0.0002	0.0068	0.0001	0.0016	0.0218	0.0107	0.0001	0.0001	0.0007	0.0008	0.0001	0.0001	0.0187	0.0004	0.0064	0.0001				
Afalou	0.0012	0.0001	0.0012	0.0001	0.0001	0.0001	0.0001	0.0001	0.0001	0.0001	0.0001	0.0001	0.0001	0.0001	0.0001	0.0001	0.0157	0.0001	0.0001			
Taforalt	0.0001	0.0001	0.0007	0.0004	0.0001	0.0001	0.0001	0.0010	0.0001	0.0001	0.0001	0.0001	0.0001	0.0001	0.0001	0.0001	0.0333	0.0001	0.0001	0.0018		
Nazlet Khater 2	0.0825	0.1341	0.0850	0.2392	0.1264	0.2187	0.1915	0.2894	0.0422	0.0444	0.0709	0.0701	0.0237	0.0577	0.2407	0.0747	0.4750	0.7183	0.3679	0.0911	0.4273	
Nataruk	0.0001	0.0001	0.0001	0.0001	0.0001	0.0001	0.0002	0.0028	0.0001	0.0001	0.0001	0.0001	0.0001	0.0001	0.0001	0.0001	0.0109	0.1527	0.0001	0.0001	0.0003	0.8049

Bold types: p -values > 0.05, indicating that the pairwise group difference is not significant.

Table 5. Between groups PCA – meta-populations sample. *p*-values of pairwise group differences – based on permutation testing

	Nile Valley	Sub-Saharan	Asia	Oceania	Europe	Inuit	Holocene Kenya	Pleistocene Europe	Pleistocene North Africa
Sub-Saharan	0.0001								
Asia	0.0001	0.0001							
Oceania	0.0001	0.0001	0.0004						
Europe	0.0001	0.0001	0.0003	0.0001					
Inuit	0.0001	0.0047	0.0001	0.0001	0.0001				
Holocene Kenya	0.0001	0.0001	0.0001	0.0001	0.0001	0.0001			
Pleistocene Europe	0.0001	0.0003	0.0001	0.0003	0.0001	0.0188	0.0001		
Pleistocene North Africa	0.0001	0.0001	0.0001	0.0001	0.0001	0.0001	0.0001	0.0001	
Nataruk	0.0001	0.0001	0.0001	0.0001	0.0001	0.0001	0.2109	0.0001	0.0001

Bold types: *p*-values > 0.05, indicating that the pairwise group difference is not significant.



Figure 1. Four of the mandibles from the site of Nataruk (West Turkana, Kenya) showed in norma lateralis, norma facialis, norma occipitalis and normal superalis (from left to right). (A) KNM-WT 71251, (B) KNM-WT 71253, (C) KNM-WT 71254, (D) KNM-WT 71255. The mandibles are scaled in relation to each other.

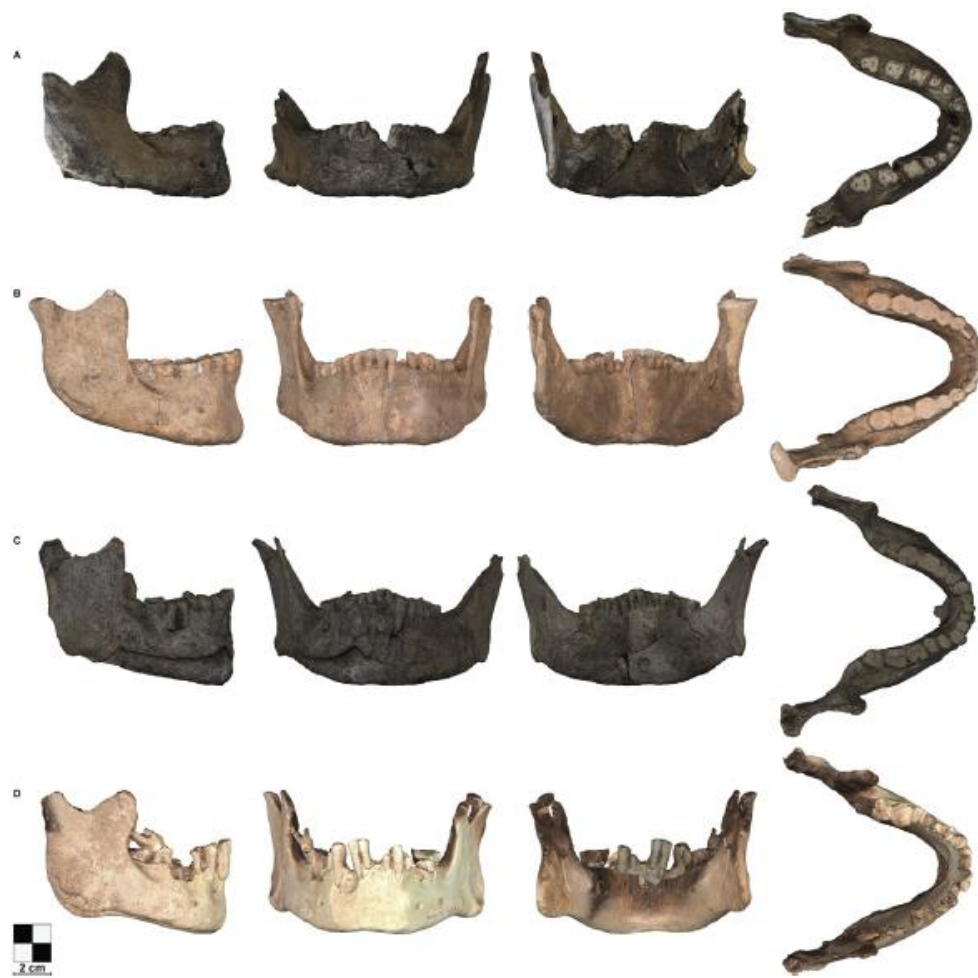


Figure 2. Four of the mandibles from the site of Nataruk (West Turkana, Kenya) showed in norma lateralis, norma facialis, norma occipitalis and norma superalis (from left to right). (A) KNM-WT 71256, (B) KNM-WT 71257, (C) KNM-WT 71263, (D) KNM-WT 71264. The mandibles are scaled in relation to each other. Norma lateralis is reversed for KNM-WT 71256.

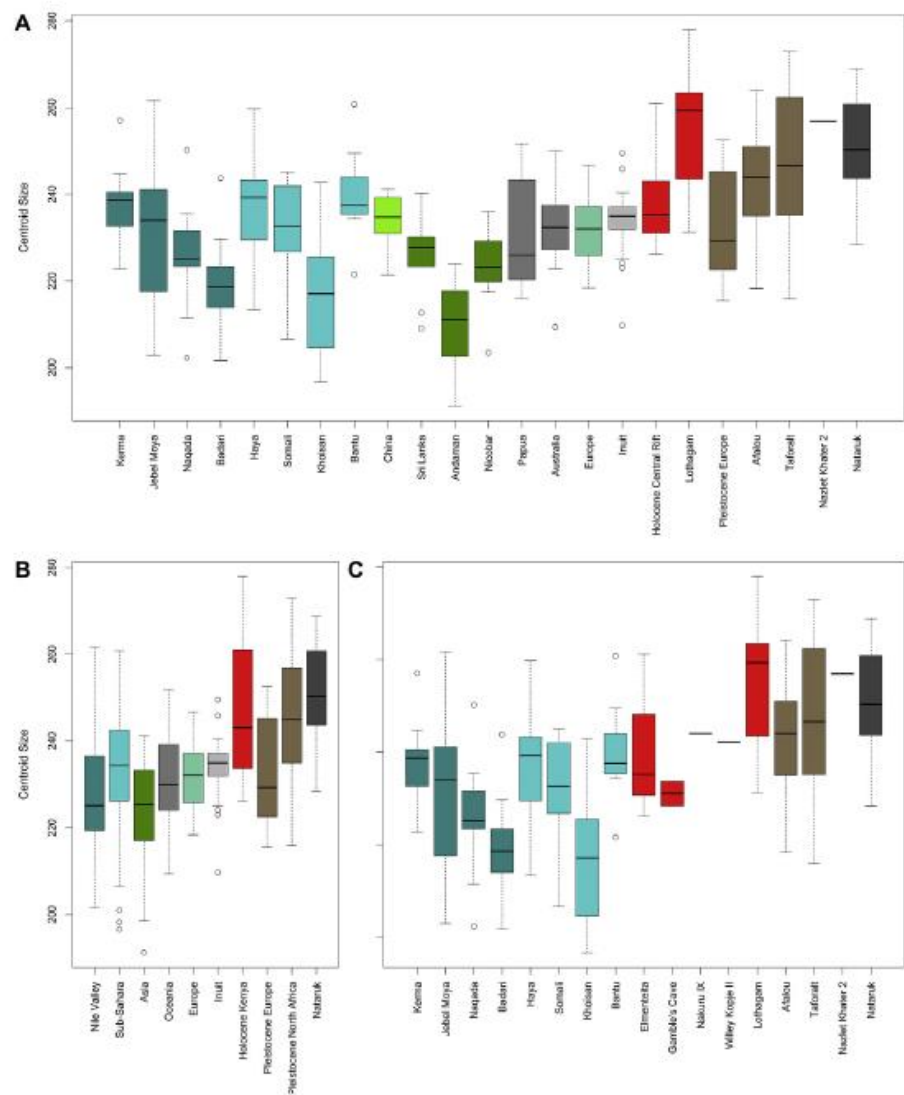


Figure 3. Boxplots showing centroid size according to the three different grouping of our sample. (A) worldwide populations, (B) worldwide meta-populations, and (C) African populations. The size of the Nataruk mandible is similar to Pleistocene specimens, and to the Lothagam sample.

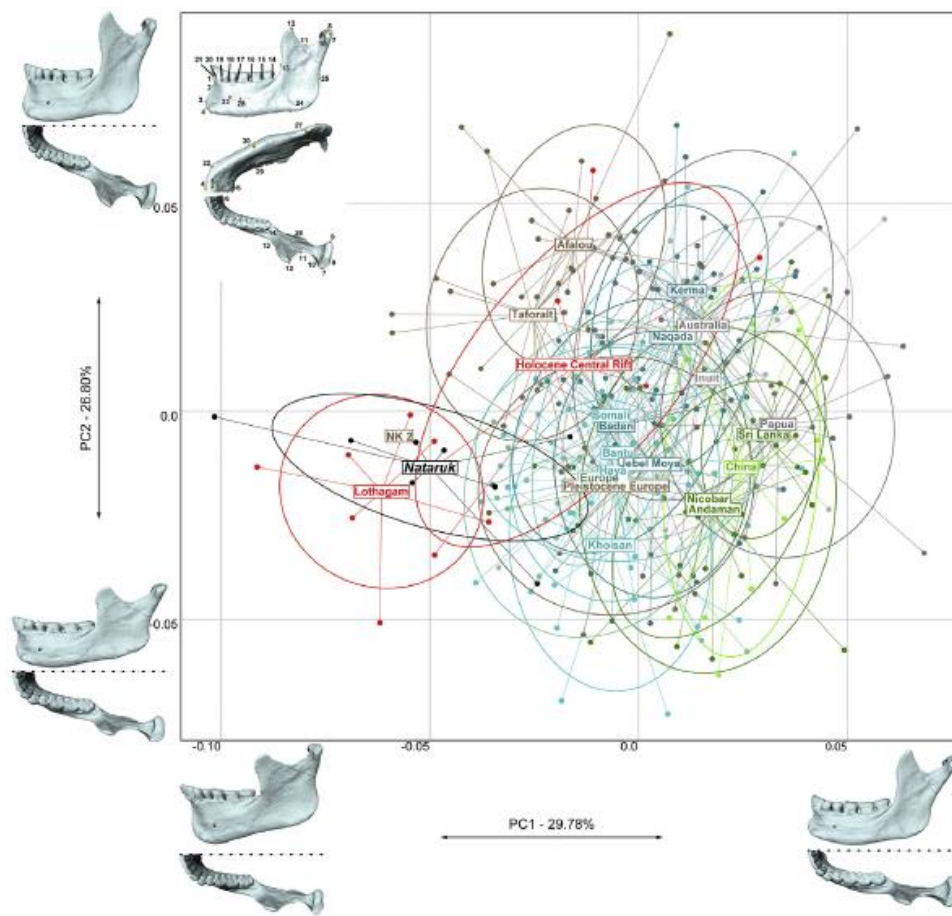


Figure 4 bgPCA showing the variation in shape within the mandibular sample grouped per worldwide populations. The ellipses represent the 90% confidence interval for the estimated distribution of the specimens of each population. Each specimen is linked to the centroid of its group of origin. The Nataruk specimens are closer in shape to the Lothagam (red) and late Pleistocene Afalou and Taforalt (brown) specimens. NK2 stands for Nazlet Khater 2. (For interpretation of the references to color in this figure legend, the reader is referred to the Web version of this article.)

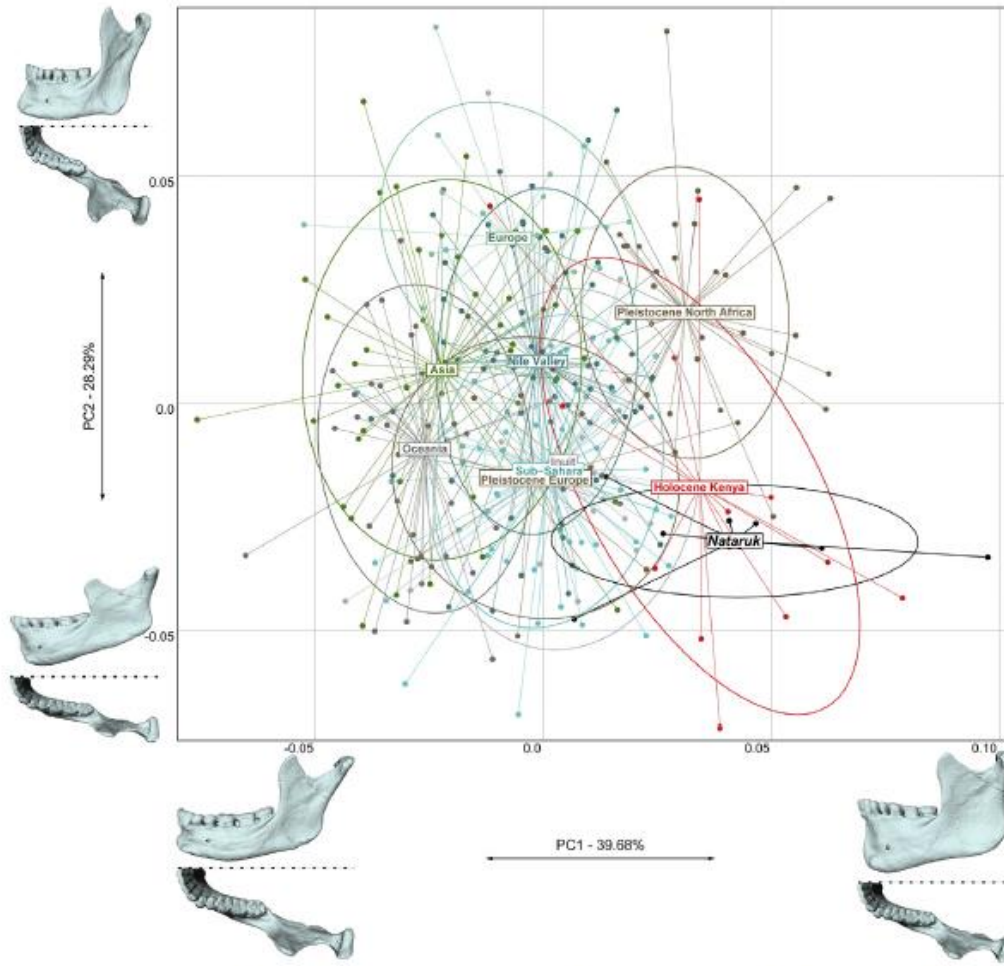


Figure 5. bgPCA showing the variation in shape within the mandibular sample grouped per worldwide meta-populations. The ellipses represent the 90% confidence interval for the estimated distribution of the specimens of each population. Each specimen is linked to the centroid of its group of origin. The Nataruk specimens are closer in shape to the Kenyan Holocene (red) and North Africa Pleistocene (brown) specimens. (For interpretation of the references to color in this figure legend, the reader is referred to the Web version of this article.)

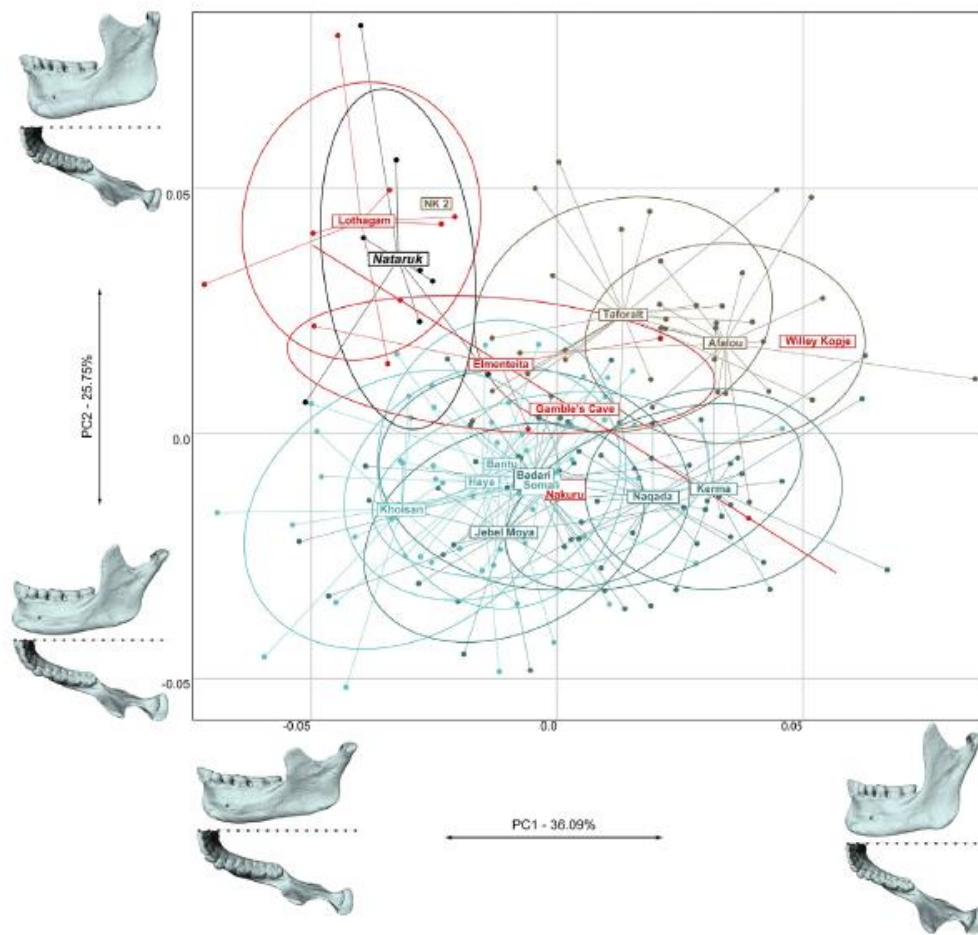


Figure 6. bgPCA showing the variation in shape within the mandibular sample grouped per African populations. The ellipses represent the 90% confidence interval for the estimated distribution of the specimens of each population. Each specimen is linked to the centroid of its group of origin. The Nataruk specimens are closer in shape to the Lothagam (red) and Nazlet Khater 2 (i.e., NK2, brown) specimens. (For interpretation of the references to color in this figure legend, the reader is referred to the Web version of this article.)

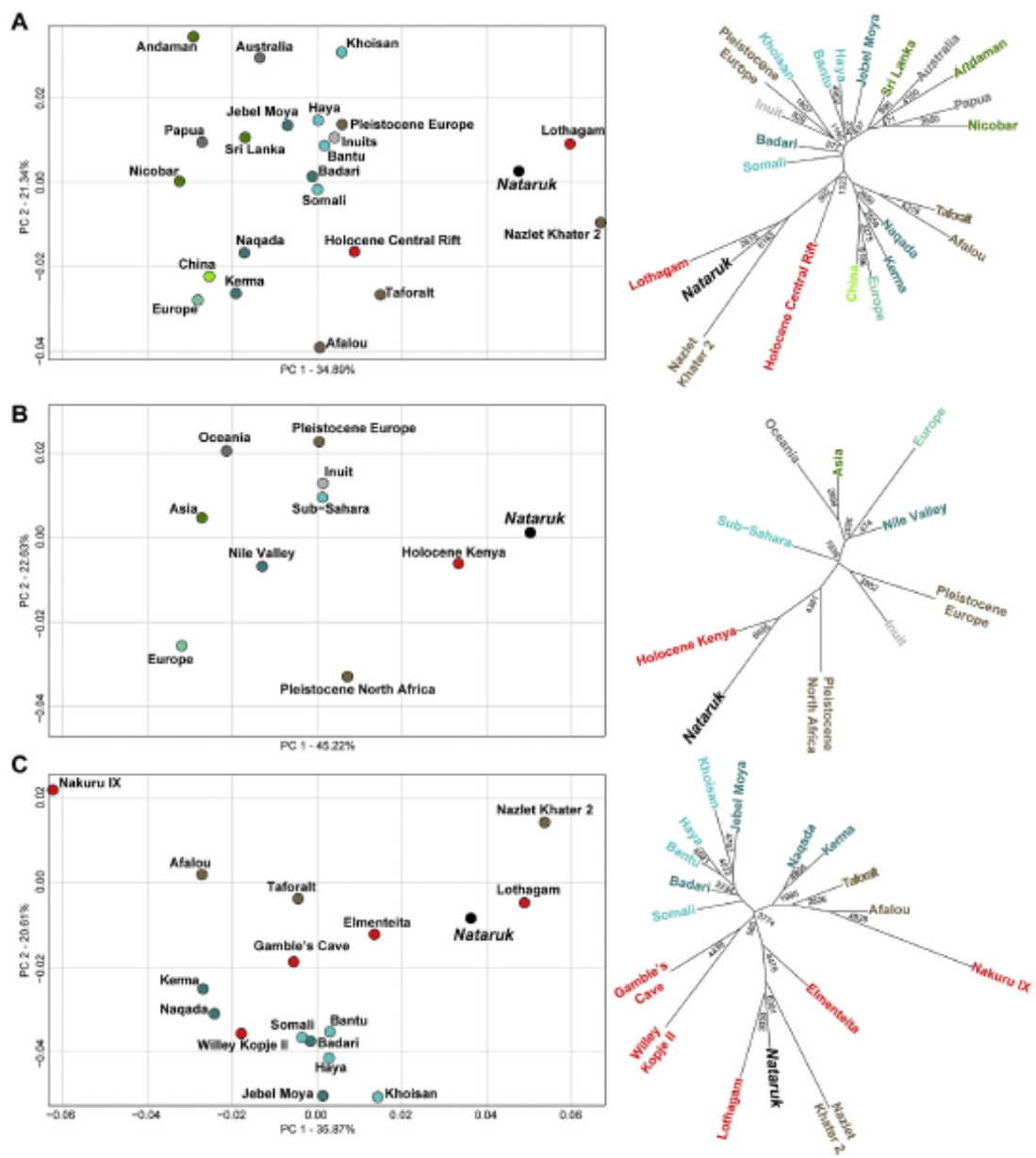


Figure 7. PCAs run on the mean shape of each population and associated unrooted Neighbor-joining trees with a 10,000 replications bootstrap. (A) worldwide populations, (B) worldwide meta-populations, and (C) African populations. In each tree, the Nataruk and Lothagam specimens (Holocene Kenya in 7 B) cluster together.